Detrital zircon U-Pb geochronology and Hf isotope geochemistry of Paleozoic and Triassic passive margin strata of western North America

George Gehrels and Mark Pecha
Department of Geosciences, University of Arizona, Tucson, Arizona 85721, USA

ABSTRACT

U-Pb geochronologic and Hf isotopic analyses have been conducted on detrital zircons extracted from 36 samples of Neoproterozoic through Triassic passive margin strata from western North America. The data serve as an improved reference for comparison with inboard strata that accumulated on the North American craton and outboard strata belonging to potentially displaced Cordilleran terranes. As expected, this reference documents significant variations in ages and Hf isotope compositions both north-south and also through time. The data also provide insights into the provenance of Cordilleran passive margin strata. During Neoproterozoic, Cambrian, and Early–Middle Devonian time, most grains were shed from relatively local basement rocks and from Mesoproterozoic clastic strata containing 1.2–1.0 Ga grains that originated in the Grenville orogen. This pattern was interrupted during Ordovician time, when much of the Cordilleran margin was blanketed by detritus shed from the northern Canadian Shield. Beginning in Late Devonian time, and continuing through late Paleozoic and Triassic time, most regions were dominated by locally derived detritus (largely recycled from underlying strata), but also received 0.7–0.4 Ga grains that were shed from the Franklinian, Caledonian, Appalachian, and Ouachita-Marathon orogens. This pattern is complicated in southern transects as a result of mid-Paleozoic emplacement of off-shelf assemblages onto the continental margin (e.g., Antler orogeny) and construction of Permo-Triassic magmatic arcs along the margin. Our data also provide a robust record of the crustal evolution of western North America, with significant production of juvenile crust during late Archean (3.0–2.5 Ga) and Paleoproterozoic (1.78–1.6 Ga) time and phases of mainly crustal reworking at 2.0–1.78, 1.5–1.3, 1.2–1.0, and 0.6–0.2 Ga. This history is somewhat different from that of other continents, with western Laurentia comprising a greater overall proportion of juvenile crust, punctuated by greater degrees of crustal reworking between 2.2 and 1.78 Ga and 0.3–0.2 Ga.

INTRODUCTION

U-Pb ages of detrital zircon grains are typically used to determine provenance, constrain the maximum depositional age of the host strata, characterize the source from which zircons were shed, and/or characterize the host strata for comparison with other units (Gehrels, 2000; Fedo et al., 2003). The latter comparisons can provide information on a range of scales, from establishing local stratigraphic correlation to reconstructing plate configurations. Characterizing the detrital zircon age distribution of a sedimentary unit is commonly referred to as establishing a detrital zircon fingerprint (Ross and Parrish, 1991), reference (Gehrels et al., 1995), barcode (Sircombe, 2000; Link et al., 2005), or chronofacies (Lawton et al., 2010).

This study attempts to characterize the ages and Hf isotope compositions of detrital zircons that accumulated along the western margin of North America from Neoproterozoic through Triassic time (Fig. 1). A similar detrital zircon reference was originally reported by Gehrels et al. (1995), based on U-Pb analysis by isotope-dilution thermal ionization mass spectrometry (ID-TIMS), and has been used in many subsequent analyses to constrain provenance, paleogeography, and displacement of outboard terranes. The original data set is significantly enhanced herein by analysis of a larger number of grains per sample, random selection of analyzed grains, and addition of Hf isotope data.

We have re-analyzed the original 23 samples reported by Gehrels et al. (1995), and an additional 13 samples that were analyzed in subsequent studies, utilizing laser-ablation inductively coupled plasma mass spectrometry (LA-ICPMS) and updated analytical methods. Primary improvements in methodology are that (1) ~200 grains were analyzed for U-Pb age for most samples, (2) zircon grains were selected at random from a representative split of all available grains, and (3) cathodoluminescence (CL) images were used to optimize analysis locations. We have also conducted Hf isotopic measurements on ~50 representative grains per sample in an effort to complement the geochronologic data with petrogenetic information. Collectively, 6461 new U-Pb ages and 1665 Hf isotope analyses are reported.
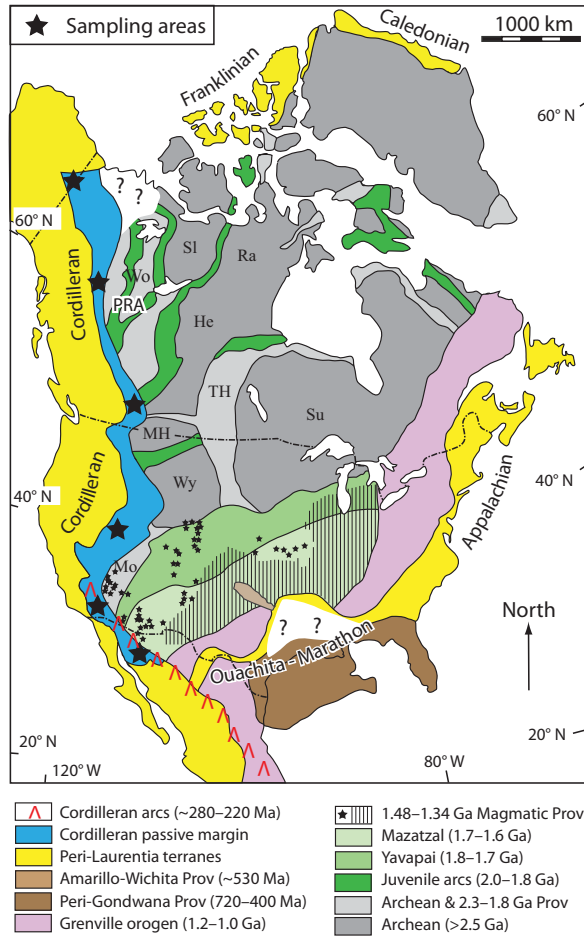
SAMPLES ANALYZED

Thirty-six samples have been studied, as shown schematically on Figure 2 and described below. Location information for each sample is provided in Supplemental Tables 1–6 in the Supplemental Table File[1], and detailed sample descriptions are provided in the references cited in these tables.

Two samples were analyzed from eastern Alaska, including the Lower Cambrian Adams Argillite and the Upper Devonian Nation River Formation. Both samples clearly accumulated on the cratonal margin of North America, although the Nation River Formation also received detritus from a peri-cratonic source terrane to the north (Gehrels et al., 1999; Beranek et al., 2010; Anfinson et al., 2011).

---

[1]Supplemental Table File. Zipped file containing 13 Excel table files. Table 1: Alaska U-Pb data. Table 2: Northern British Columbia U-Pb data. Table 3: Southern British Columbia U-Pb data. Table 4: Nevada-Utah U-Pb data. Table 5: Southern California U-Pb data. Table 6: Sonora U-Pb data. Table 7: Hf standard data. Table 8: Alaska Hf data. Table 9: Northern British Columbia Hf data. Table 10: Southern British Columbia Hf data. Table 11: Nevada-Utah Hf data. Table 12: Southern California Hf data. Table 13: Sonora Hf data. If you are viewing the PDF of this paper or reading it offline, please visit http://dx.doi.org/10.1130/GES00889.S1 or the full-text article on www.gsapubs.org to view the Supplemental Table File.

Figure 1. Location of sample transects (stars) relative to first-order crustal provinces (Prov) of North America (adapted from Hoffman [1989], Whitmeyer and Karlstrom [2007], Gehrels et al., [2011]). PRA—Peace River Arch region; Mo—Mojave province; Wy—Wyoming province; MH—Medicine Hat province; Su—Superior province; TH—Trans-Hudson province; Ra—Rae province; He—Hearne province; Sl—Slave province; Wo—Wopmay province.

Figure 2. Schematic diagram showing stratigraphic units studied and approximate ages. Valmy, Vinini, and Aliso belong to off-shelf assemblages. N River—Nation River; M Wilson—Mount Wilson; HT Creek—Horsethief Creek; Wd Cnyn—Wood Canyon; Mina Mex—Mina Mexico.

From northern British Columbia, samples have been analyzed from the Lower Cambrian Atan Group, Lower or Middle Ordovician Monkman Formation, Lower or Middle Devonian Wokkpash Formation, Permian Kindle Formation, and Middle or Upper Triassic Liard Formation (Ross et al., 1997; Gehrels and Ross, 1998). These samples record influence from both the North American craton and the Franklinian orogen to the north (Beranek et al., 2010; Anfinson et al., 2011).

From southern British Columbia, samples include the Neoproterozoic Horsethief Creek Group, Lower Cambrian Hamill Group, Middle or Upper Ordovician Mount Wilson Formation, Pennsylvanian Spray Lakes Group, and Upper Triassic Whitehorse Formation (Ross et al., 1997; Gehrels and Ross, 1998). U-Pb ages have also been determined from the Upper Devonian Sassenach Formation (Stevenson et al., 2000).

From Nevada and Utah, passive margin strata include the Lower Cambrian Osgood Mountains Quartzite, Middle Ordovician Eureka Quartzite, Middle Devonian Oxyoke Canyon Sandstone, Upper Triassic Osobb Formation, and Upper Triassic Chinle Formation (studied by Gehrels and Dickinson, 1995), as well as the Neoproterozoic Caddy Canyon Quartzite, Neoproterozoic Mutual Formation, and Neoproterozoic to Lower Cambrian Geertsen Canyon Quartzite (studied by Stewart et al., 2001). Samples from off-shelf assemblages include the Lower or Middle Ordovician Vinini Formation (Gehrels et al., 2000a) and the Ordovician Valmy Formation (Smith and Gehrels, 1994). We have also analyzed samples from Mississippian strata of the Tonka Formation and Pennsylvanian strata of the Battle Formation, which are widely interpreted to have been shed from off-shelf strata (e.g., Valmy and Vinini Formations) exposed in the Antler highlands to the west (Burchfiel et al., 1992; Gehrels and Dickinson, 1995, 2000).

We have also analyzed three samples from southern California that were first reported by Stewart et al. (2001). Included are two samples of the Neoproterozoic to Lower Cambrian Wood Canyon Formation and one sample of the Lower Cambrian Zabriskie Quartzite.

From Sonora, samples from shelf-facies strata that were described originally by Gehrels and Stewart (1998) include the Lower Cambrian Proveedora Quartzite, Middle or Upper Ordovician Quartzite of Sierra Lopez, Upper Devonian Quartzite of Cerro Pollo, and Lower Permian Quartzite of Sierra Santa Teresa. Additional units from the original study include off-shelf strata of the Middle Ordovician Quartzite of Sierra El Aliso and Upper Triassic strata of the Barranca Group that accumulated on Paleo-

zoic off-shelf strata in proximity to the Triassic magmatic arc built along the Cordilleran margin (Gehrels and Stewart, 1988). We have also re-analyzed two samples reported by Poole et al. (2008), including deep-water strata of the Upper Devonian Los Pozos Formation and Lower Permian strata of the Mina Mexico Formation. A final sample is from the Upper Triassic Antimonio Formation, which accumulated in a basinal setting outboard of the Triassic magmatic arc (González-León et al., 2005).

METHODS

Analyses reported herein were conducted by LA-ICPMS at the Arizona LaserChron Center (Tucson, Arizona). Data were collected during several different sessions from 2006 to 2011, first utilizing a GVI Isoprobe connected to a New Wave UP193 HE laser, second with a Nu Plasma HR multicollector ICPMS connected to a New Wave UP193 HE laser, and finally with the Nu ICPMS connected to a Photon Machines Analyte G2 excimer laser. Details of our procedures for collecting, analyzing, and interpreting the data are described in Supplemental File 1[2].

U-Pb Geochronology

U-Pb ages from each transect are shown on normalized probability density plots (PDPs) in Figures 3–10. The geochronologic data, Pb/U concordia diagrams, PDPs, and lists of age groups and peak ages are all provided in Supplemental Tables 1–6 in the Supplemental Table File (see footnote 1).

Figures 3 and 4 provide a comparison between the ID-TIMS data originally presented for these samples and our LA-ICPMS ages. Figure 3 shows data for Cambrian, Devonian, Pennsylvanian, and Triassic samples, which yield similar groups of ages. Figure 4 shows ages for Ordovician strata, which commonly differ from ages in older and younger strata. Age data from the two different methods are highly compatible, with the main age groups apparent in both data sets. There are also significant differences, however, as outlined below.

One of the significant differences in the two data sets is that the ID-TIMS analyses yield more restricted age ranges than the LA-ICPMS analyses. This is due largely to the higher precision of ID-TIMS, with average uncertainties of 0.4% (1σ) for all ID-TIMS ages compared with 1.9% (1σ) for all LA-ICPMS ages. A second

factor is the greater number of LA-ICPMS ages per sample (~7×, on average), which results in a broader range of observed ages.

A second difference is the variation in proportions of age groups, which results mainly from differing grain-selection procedures. For ID-TIMS, crystals were selected from each color and morphology group, regardless of the abundance of grains composing each group. For LA-ICPMS, grains were selected at random from the full population of grains. The procedure used for LA-ICPMS analyses generates a more representative age distribution given that grains are selected at random; the following discussions accordingly rely entirely on LA-ICPMS ages.
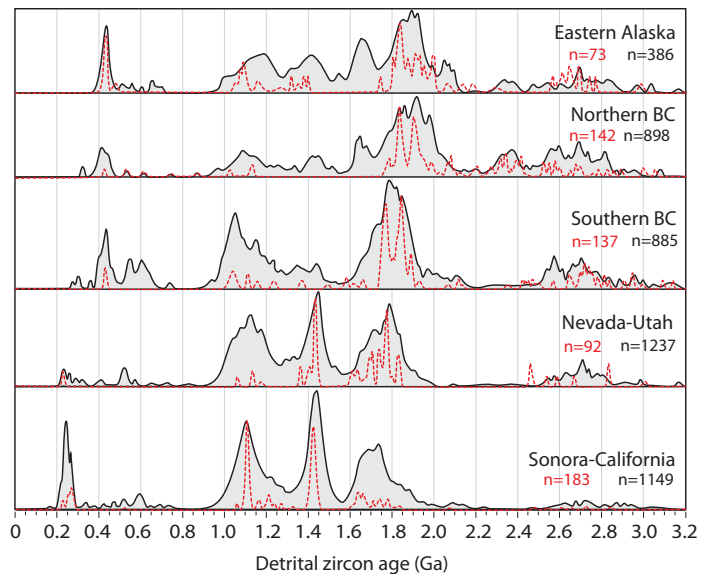

Figure 3. Probability density plots showing ages from strata of Neoproterozoic, Cambrian, Devonian, late Paleozoic, and Triassic age. Isotope-dilution thermal ionization mass spectrometry data shown with red lines; laser-ablation inductively coupled plasma mass spectrometry data shown with black lines. Number of constituent analyses is indicated. BC—British Columbia.
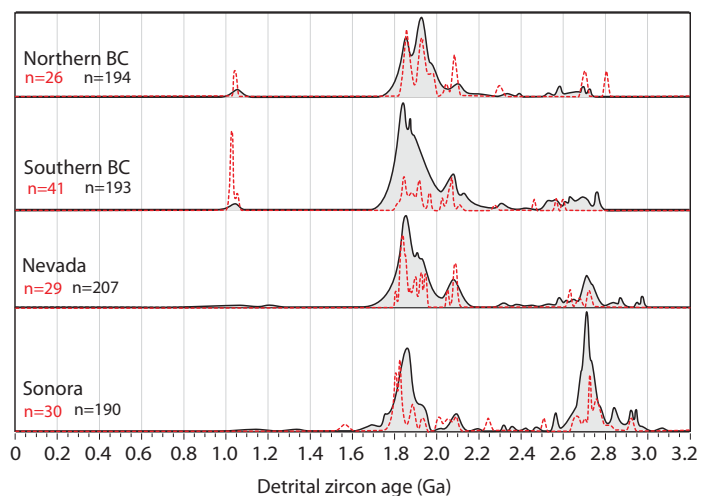

Figure 4. Probability density plots comparing data from isotope-dilution thermal ionization mass spectrometry (red lines) with data from laser-ablation inductively coupled plasma mass spectrometry for Ordovician strata. Number of constituent analyses is indicated. BC—British Columbia.

Hf Isotope Analysis

Thirty-three of the 36 samples have been analyzed for Hf isotopes; three contained grains that were too small for analysis even with a 30 μm beam diameter. An average of 50 analyses were conducted per sample, with grains selected to represent each of the main age groups and to avoid crystals with discordant or imprecise ages. CL images were utilized (see Supplemental File 2[3]) to determine pit locations for all analyses. Hf analyses were conducted on top of the U-Pb analysis pits in most cases to ensure that at least the initial Hf isotopic data were determined from the same domain as the U-Pb age. Supplemental Table 7 in the Supplemental Table File (see footnote 1) reports all analyses of Hf standards, whereas Supplemental Tables 8–13 in the Supplemental Table File (see footnote 1) present Hf isotopic data and Hf-evolution plots for each sample.

Hf data are presented on Hf-evolution diagrams (Figs. 5–10) that show $\varepsilon Hf_{(t)}$ values at the time of crystallization. Measurement precision is shown as the average uncertainty for all analyses presented on each diagram, expressed at 2σ. External precision is estimated at ±2 epsilon units given that nearly all session averages of zircon standards are within 2 epsilon units of the reported values (Bahlburg et al., 2009). Reproducibility is estimated at ~3.1 epsilon units based on the standard deviation (expressed at 2σ) of each set of standard analyses. Following Bahlburg et al. (2011), $\varepsilon Hf_{(t)}$ values that are within 5 units of depleted mantle (DM) are referred to as juvenile in composition, values between and 5 and 12 units below DM are considered intermediate, and values >12 units below DM are considered evolved.

To assist with interpretation, Figures 5–10 show arrows that indicate the Hf isotopic evolution of typical felsic crust, assuming a $^{176}Lu/^{177}Hf$ ratio of 0.0093 (Vervoort and Patchett, 1996; Amelin et al., 1999; Bahlburg et al., 2011). Analyses that lie along a Hf-evolution trajectory are interpreted to record successive melting events of crust that may have been extracted from the mantle at the time of intersection with DM. Depleted mantle model ages for individual analyses are not presented, however, because of uncertainties in Hf isotopic evolution prior to zircon crystallization, as well as uncertainties in the evolution of CHUR (chondritic uniform reservoir) and DM (e.g., Vervoort, 2011). Yellow vertical bands on Figures 5–10 enclose

---

[3]Supplemental File 2. CL image file (238 pages). If you are viewing the PDF of this paper or reading it offline, please visit http://dx.doi.org/10.1130 /GES00889.S3 or the full-text article on www.gsapubs .org to view Supplemental File 2.

---

analyses of approximately similar age that have a range of Hf isotopic composition. Such arrays are interpreted as mixtures of crustal components of variable Hf isotope composition, with involvement of juvenile (more radiogenic, mantle-derived) material indicated by analyses with juvenile $\varepsilon Hf_{(t)}$ values.

It should be noted that the Hf data presented herein are not of ideal precision due to three different factors. First is the small size of zircon grains in many samples, which required analysis of all grains in such samples (and of standards on the same mounts) with a small (30 μm) laser beam. Second, data acquired with our first laser system had large measurement uncertainties due to uneven energy distribution and irregular pit geometry. Data collected with our second laser system, used toward the end of the study, has significantly better internal precision. Third are several aspects of our analytical methodology that sacrifice internal precision to improve accuracy:

(1) Hf analysis pits are located on top of U-Pb analysis pits so that at least the initial Hf measurements are likely from the same domain as the U-Pb age. This ensures connection between the U-Pb age and the initial Hf isotope data but results in somewhat lower internal precision.

(2) Uncertainties are calculated using all data acquired during an acquisition, rather than only a portion of the analysis with the best precision. This generates uncertainties that are representative of all of the material analyzed, but are commonly larger than if only part of an analysis is selected.

(3) Our mass spectrometer is tuned (by adjusting gas flows and beam focusing) such that the measured Hf isotope data are corrected for only measured mass-dependent fractionation and isotopic interference. These tune settings commonly yield slightly lower sensitivity, which results in lower precision, but alleviates the need to apply any additional correction factors.

U-Pb AGES AND Hf ISOTOPIC INFORMATION

Eastern Alaska

Our two samples from eastern Alaska yield similar sets of ages (PDPs on Fig. 5; Supplemental Table 1 in the Supplemental Table File [see footnote 1]), with dominant age groups of 1.97–1.76, 1.72–1.60, 1.48–1.30, and 1.26–0.98 Ga. There are also subordinate groups of Achean age, 2.10–2.03 Ga, and 0.72–0.50 Ga. In addition, 0.47–0.40 Ga grains are present in the Nation River Formation.

The Hf data from these two samples are also similar, with mostly intermediate and evolved

$\varepsilon Hf_{(t)}$ values for >1.3 Ga grains and mostly intermediate and juvenile compositions for <1.3 Ga grains (Fig. 5; Supplemental Table 8 in the Supplemental Table File [see footnote 1]). One set of 1.8–1.3 Ga grains is interpreted to lie along a Hf-evolution trajectory (gray band on Fig. 5) that records episodic remelting of crust that originated during Paleoproterozoic time. Vertical arrays (yellow bands) are interpreted to record reworking of mainly evolved and intermediate crust at 2.1–1.8 Ga, and mixing of mainly intermediate and juvenile crust at 1.3–1.0 Ga and 0.7–0.4 Ga.

Northern British Columbia

Samples from northern British Columbia record two very different age distributions (PDPs of Fig. 6; Supplemental Table 2 in the Supplemental Table File [see footnote 1]). Cambrian though Devonian samples yield dominantly 2.12–1.76 Ga grains and subordinate age groups of 2.73–2.54 and 2.42–2.27 Ga. The Ordovician Monkman Formation also contains several grains of 1.12–1.01 Ga. The Kindle (Permian) and Liard (Triassic) Formations exhibit age groups that are quite different from underlying strata, with primary age groups of 2.85–2.64, 2.03–1.60, 1.54–1.37, 1.20–1.02, and 0.48–0.38 Ga (Fig. 6).

Hf isotopic data for >1.3 Ga grains are similar to those from the samples from eastern Alaska, with mostly intermediate and evolved compositions (Fig. 6; Supplemental Table 9 in the Supplemental Table File [see footnote 1]). $\varepsilon Hf_{(t)}$ values for <1.3 Ga grains are also mostly intermediate to evolved, in contrast to the more juvenile values from young grains in eastern Alaska. One set of 1.7–1.0 Ga grains is interpreted to lie along a Hf-evolution trajectory (gray band on Fig. 6) that records episodic remelting of Paleoproterozoic crust. Vertical arrays are interpreted to record reworking of evolved, intermediate, and possibly juvenile crust at 2.1–1.8 Ga, mixing of juvenile to moderately evolved crust at 1.8–1.6 Ga, and mixing of intermediate and evolved (some highly evolved) crust at 1.2–1.0 Ga and 0.60–0.40 Ga (Fig. 6; Supplemental Table 9 in the Supplemental Table File [see footnote 1]).

Southern British Columbia

Strata from southern British Columbia display three different age distributions (Fig. 7; Supplemental Table 3 in the Supplemental Table File [see footnote 1]). The Horsethief Creek and Hamill Groups yield grains that are mainly 1.94–1.65 Ga, with a subordinate population of 3.01–2.50 Ga grains. The Ordo-
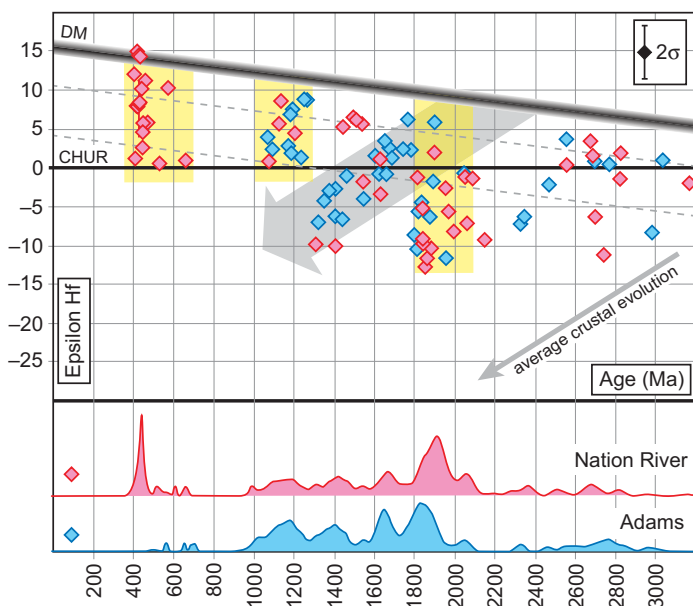
Figure 5. U-Pb and Hf data and interpretations for samples from eastern Alaska. Lower curves are probability density plots of U-Pb ages, normalized such that each curve contains the same area. Analyses (with number of U-Pb analyses) are from the Lower Cambrian Adams Argillite (n = 198) and the Upper Devonian Nation River Formation (n = 187). Upper plot shows εHf$_{(t)}$ values for each sample. The average measurement uncertainty for all analyses (upper right) is shown at the 2σ level. Reference lines on the Hf plot are as follows: DM—depleted mantle, calculated using ^{176}Hf/^{177}Hf$_0$ = 0.283225 and ^{176}Lu/^{177}Hf$_0$ = 0.038512 (Vervoort and Blichert-Toft, 1999); CHUR—chondritic uniform reservoir, calculated using ^{176}Hf/^{177}Hf = 0.282785 and ^{176}Lu/^{177}Hf = 0.0336 (Bouvier et al., 2008); gray dashed lines separate fields described as juvenile (0–5 epsilon units below DM), intermediate (5–12 epsilon units below DM), and evolved (>12 epsilon units below DM) following Bahlburg et al. (2011). Gray arrows show interpreted crustal evolution trajectories assuming present-day ^{176}Lu/^{177}Hf = 0.0093 (Vervoort and Patchett, 1996; Vervoort et al., 1999; Bahlburg et al., 2011). Yellow vertical bands indicate interpreted mixing of materials with different Hf isotope composition.

vician Mount Wilson Formation is dominated by slightly older 2.00–1.75 Ga grains, with subordinate groups at 2.78–2.52, 2.11–2.04, and 1.08–0.99 Ga. Devonian and younger strata have dominant age groups of 1.93–1.61 and 1.25–0.98 Ga and subordinate age groups at 2.85–2.51, 2.14–1.95, 1.47–1.31, 0.66–0.52, and 0.49–0.39 Ga.

The Hf data are similar to the results for northern British Columbia, with vertical arrays interpreted to record mixing of mostly intermediate to evolved crustal materials at 1.2–1.0 Ga and 0.60–0.40 Ga and incorporation of juvenile and evolved materials at 2.2–1.78 and 1.5–1.3 Ga (Fig. 7; Supplemental Table 10 in the Supplemental Table File [see footnote 1]).

Nevada and Utah

Strata from Nevada and Utah yield several different age distributions, as shown in Figure 8 (Supplemental Table 4 in the Supplemental Table File [see footnote 1]). Neoproterozoic samples yield primarily 1.24–0.99 Ga ages, with subordinate groups at 2.85–2.59, 1.99–1.74, and 1.47–1.32 Ga. Cambrian (and perhaps latest Neoproterozoic) samples have a dominant age group of 1.89–1.70 Ga and less abundant groups at 2.80–2.53, 1.50–1.36, and 1.24–1.00 Ga. The next set of similar samples includes Ordovician shelf-facies strata (Eureka Quartzite), Ordovician off-shelf-facies strata (Valmy Formation), and Mississippian (Tonka

Formation) and Pennsylvanian (Battle Formation) strata of the Antler overlap assemblage. This set is characterized by a single dominant group of 1.98–1.75 Ga grains and subordinate populations at 2.78–2.57 and 2.12–2.05 Ga. An additional sample of Ordovician off-shelf strata (Vinini Formation) yields a very different age distribution from the other Ordovician strata, with dominant age groups of 1.86–1.68 and 0.52–0.46 Ga. The Devonian Oxyoke Formation yields an age distribution that is similar to Cambrian strata, with main age groups of 1.82–1.60 and 1.52–1.38 Ga. Finally, the two Triassic samples (Chinle and Osobb Formations) yield age groups of 1.85–1.62, 1.49–1.39, 1.20–0.97, 0.58–0.49, and 0.33–0.21 Ga.

Samples from Nevada and Utah yield a broad range of εHf$_{(t)}$ values from juvenile to highly evolved (Fig. 8; Supplemental Table 11 in the Supplemental Table File [see footnote 1]). First-order patterns are that >2.5 Ga and 1.8–1.0 Ga grains are mostly juvenile and intermediate, whereas 2.3–2.0 and <1.0 Ga grains are mostly intermediate and evolved. Vertical arrays are interpreted to record mixing of juvenile and highly evolved crust between 2.1 and 1.78 Ga, and with less evolved crust after 1.78 Ga. Exceptions to this are 1.1–1.0 Ga grains in the Eureka, Valmy, and Battle formations and 0.3–0.2 Ga grains in the Chinle Formation that also incorporated highly evolved crust.

Southern California

The three samples from southern California yield two different age distributions (Fig. 9; Supplemental Table 5 in the Supplemental Table File [see footnote 1]). One of the samples from the Wood Canyon Formation is dominated by zircons that are 1.2–1.0 Ga, whereas the other sample of Wood Canyon Formation and the Zabriskie Quartzite yield three prominent age groups of 1.92–1.60, 1.51–1.36, and 1.27–1.05 Ga.

Hf isotope compositions from these samples are almost entirely juvenile and intermediate (Fig. 9; Supplemental Table 12 in the Supplemental Table File [see footnote 1]). Three vertical arrays are interpreted to record mixing of juvenile and intermediate crustal components. Wooden et al. (2013) reported very similar U-Pb ages and Hf isotopic compositions from the Wood Canyon and Zabriskie formations in southern California (Fig. 9).

Sonora

Five different age groups are apparent in the age distributions from Sonoran samples (Fig. 10; Supplemental Table 6 in the Supplemental Table
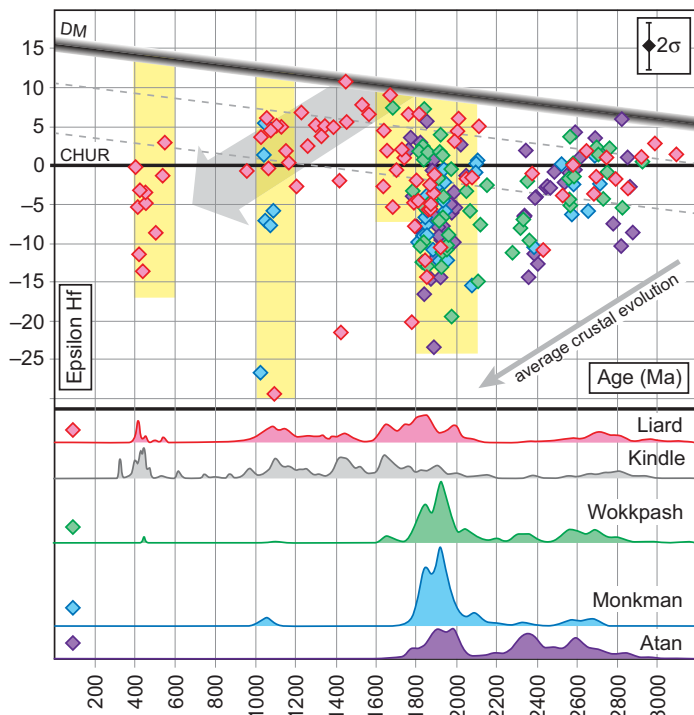
Figure 6. U-Pb and Hf data and interpretations for samples from northern British Columbia. Analyses are from the Lower Cambrian Atan Group (n = 201), Lower or Middle Ordovician Monkman Formation (n = 194), Lower or Middle Devonian Wokkpash Formation (n = 203), Permian Kindle Formation (n = 195), and Middle or Upper Triassic Liard Formation (n = 299). Diagrams and symbols are as in Figure 5.
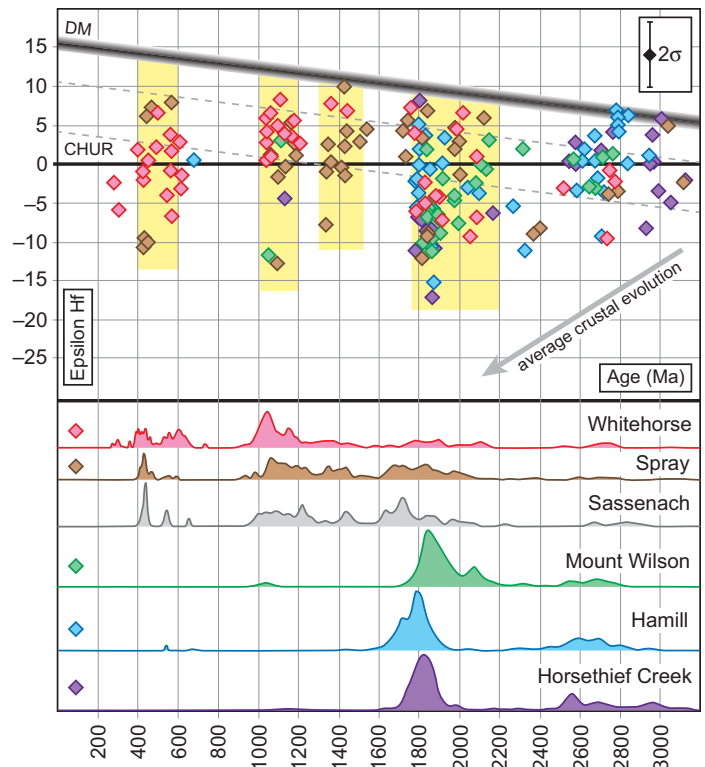
Figure 7. U-Pb and Hf data and interpretations for samples from southern British Columbia. Analyses are from the Neoproterozoic Horsethief Creek Group (n = 195), Lower Cambrian Hamill Group (n = 196), Middle or Upper Ordovician Mount Wilson Formation (n = 193), Upper Devonian Sassenach Formation (n = 100), Pennsylvanian Spray Lakes Group (n = 198), and Upper Triassic Whitehorse Formation (n = 196). Diagrams and symbols are as in Figure 5.

File [see footnote 1]). Oldest is the Proveedora Quartzite, which yields three dominant age groups of 1.81–1.61, 1.51–1.37, and 1.30–1.00 Ga. Two Ordovician samples yield mainly older grains, with dominant ages of 2.79–2.65 and 1.95–1.77 Ga. Two Devonian samples yield age groups of 1.87–1.59 and 1.50–1.32 Ga, with a subordinate set of 1.26–1.04 Ga grains and a few younger grains at 0.52–0.48 Ga. Age distributions from Permian strata are more varied, with age groups at 2.85–2.54, 1.93–1.60, 1.51–1.36, 1.16–0.99, and 0.63–0.31 Ga. Triassic strata are dominated by young grains, 0.29–0.21 Ga, and also have three older age groups at 1.78–1.63, 1.50–1.39, and 1.13–1.06 Ga.

Hf isotope compositions from these samples are juvenile to intermediate for Archean, 1.78–1.6, 1.5–1.4, and 1.3–1.0 Ga grains, evolved for 0.70–0.55 and 0.30–0.20 Ga grains, and highly variable from juvenile to evolved for 2.0–1.78 and 1.3–1.0 Ga grains (Fig. 10; Supplemental Table 13 in the Supplemental Table File [see footnote 1]). Vertical arrays are interpreted to record mixing of juvenile and highly evolved

crust at 2.0–1.78 and 1.3–1.0 Ga, juvenile and mostly intermediate crust during 1.78–1.6 and 1.5–1.4 Ga, and evolved to intermediate crust, with little evidence of juvenile input, during 0.70–0.55 and 0.30–0.20 Ga.

PROVENANCE IMPLICATIONS

The data from this study can be used to reconstruct provenance by comparison of the observed U-Pb ages and Hf isotope data with known values from relevant basement and igneous provinces.

Comparison with Existing U-Pb Age and Hf Data

Figure 11 provides a comparison of our detrital zircon ages (PDP curves) with the general age ranges of basement provinces and younger igneous suites of North America (vertical shaded bands; Hoffman, 1989; Whitmeyer and Karlstrom, 2007). The use of Hf isotopes for reconstructing provenance is challenging because few

Hf isotopic analyses are available for Precambrian basement provinces and younger igneous suites of North America. The available information is shown on Figure 12, with clusters of analyses enclosed in summary fields.

Paleogeographic Framework

The following sections explore provenance implications that derive from comparisons between these previously published data sets and our U-Pb and Hf isotope results. The discussion is organized by age of deposition, and is keyed to a series of reconstructions (from Ron Blakey, maps available from http://jan.ucc.nau.edu/rcb7/nam.html) that provide a paleogeographic framework for the preferred provenance interpretations (Fig. 13).

Neoproterozoic Time

The paleogeography of Laurentia was relatively straightforward during Neoproterozoic time, with passive-margin sequences accumu-
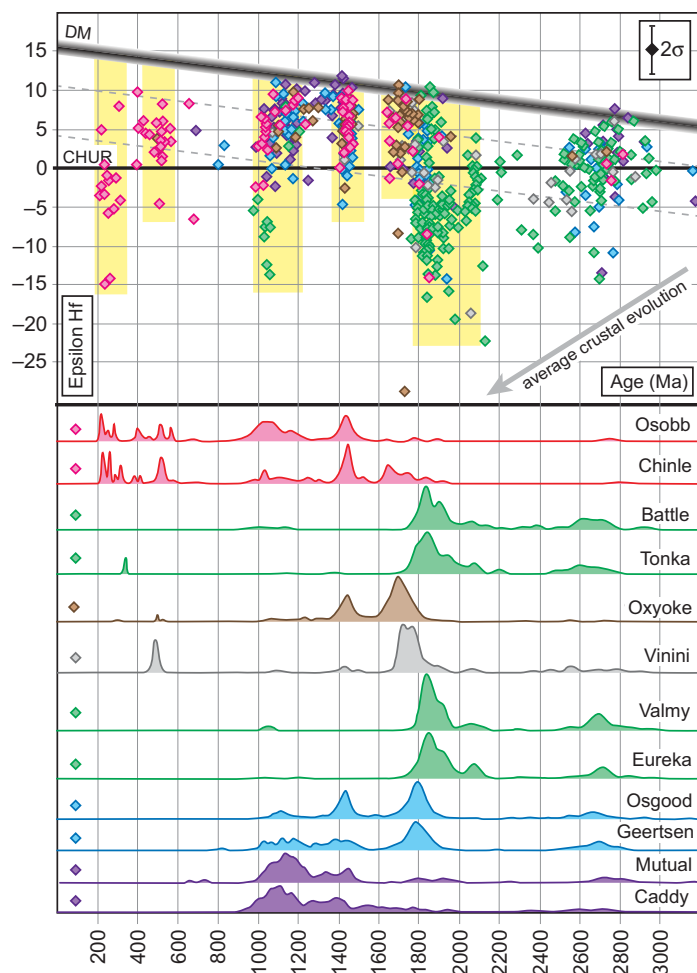
Figure 8. U-Pb and Hf data and interpretations for samples from Nevada and Utah. Analyses are from the Neoproterozoic Caddy Canyon Quartzite (n = 201), Neoproterozoic Mutual Formation (n = 213), Neoproterozoic to Lower Cambrian Geertsen Canyon Quartzite (n = 202), Lower Cambrian Osgood Mountains Quartzite (n = 209), Middle Ordovician Eureka Quartzite (n = 207), Ordovician Valmy Formation (n = 105), Lower or Middle Ordovician Vinini Formation (n = 105), Middle Devonian Oxyoke Canyon Sandstone (n = 196), Mississippian Tonka Formation (n = 105), Pennsylvanian Battle Formation (n = 101), Upper Triassic Osobb Formation (n = 106), and Upper Triassic Chinle Formation (n = 110). Diagrams and symbols are as in Figure 5.

the conclusions of Wooden et al. (2013) based on U-Pb and Hf data from strata in southern California.

Neoproterozoic strata in southern British Columbia yield a very different signature, with U-Pb ages and $\varepsilon Hf_{(t)}$ values consistent with derivation mainly from the nearby Canadian Shield (or Wyoming province; Fig. 1). There is little sign of input from Grenville-age rocks in these strata, suggesting that the Grenville clastic wedge was already removed or was never present in this area.

Strata in Nevada-Utah yield U-Pb ages and $\varepsilon Hf_{(t)}$ values that overlap with signatures to the north and south, with likely sources including the Grenville orogen, midcontinent 1.48–1.34 Ga rocks, the Mojave-Yavapai-Mazatzal provinces, and >1.8 Ga rocks of the Canadian Shield and/or Wyoming province. Mueller et al. (2007) reported similar ages and $\varepsilon Hf_{(t)}$ values from Neoproterozoic strata of the Uinta Mountain Group of northeastern Utah.

Cambrian Time

The paleogeography of Laurentia remained relatively simple during Cambrian time, with the Transcontinental Arch dominating the cratonal interior and passive-margin sequences accumulating around the margins (Sloss, 1988; Fig. 13B).

Our southernmost samples, from southern California and Sonora, yield ages and Hf isotope compositions that overlap signatures for the Mojave-Yavapai-Mazatzal provinces, 1.48–1.34 Ga midcontinent igneous rocks, and potentially overlying Mesoproterozoic strata derived from the Grenville orogen, suggesting derivation mainly from local sources (Fig. 15). Wooden et al. (2013) reached similar provenance conclusions based on U-Pb and Hf data from Cambrian strata in southern California.

Cambrian strata in Nevada have similar 1.48–1.34 Ga and 1.2–1.0 Ga components, but only minor input from the Yavapai-Mazatzal provinces. Grains with >1.8 Ga ages have Hf isotope compositions representative of the Canadian Shield and/or nearby Wyoming province. Strata in southern British Columbia are dominated by >1.8 Ga grains derived from the Canadian Shield (perhaps nearby Medicine Hat and/or Hearne provinces; Fig. 1).

Cambrian strata in northern British Columbia have ages that match well with the northwestern Canadian Shield, especially the Wopmay orogen (Ross, 1991, 2002). The lack of Hf isotopic data from the Wopmay orogen prevents a direct comparison, but our Hf data suggest that these grains were derived from mixing of evolved (Archean) and intermediate (Paleoproterozoic) crust.

lating around most of the continent (Stewart, 1976) and, at least by Early Cambrian time, emergence of the Transcontinental Arch (Sloss, 1988; Fig. 13A). Much of the craton was covered by Mesoproterozoic strata of the Grenville clastic wedge (Rainbird et al., 1992, 2012), with reworking of these strata in uplifted regions.

Samples from southern California are dominated by 1.2–1.0 Ga grains that generally overlap in age and $\varepsilon Hf_{(t)}$ values with coeval grains in other parts of North America (Fig. 14). Most grains appear to have originated in the

Grenville orogen of eastern or southern North America, with transcontinental dispersal during Mesoproterozoic time and reworking from local exposures of clastic strata during Neoproterozoic time (Rainbird et al., 1992, 2012). Grains of 1.8–1.6 and 1.48–1.34 Ga yield Hf data consistent with derivation from the Mojave-Yavapai-Mazatzal provinces (Bickford et al., 2008; Wooden et al., 2013) and 1.48–1.34 Ga granitoids of the U.S. midcontinent (Goodge and Vervoort, 2006) (Fig. 14). These provenance interpretations are consistent with
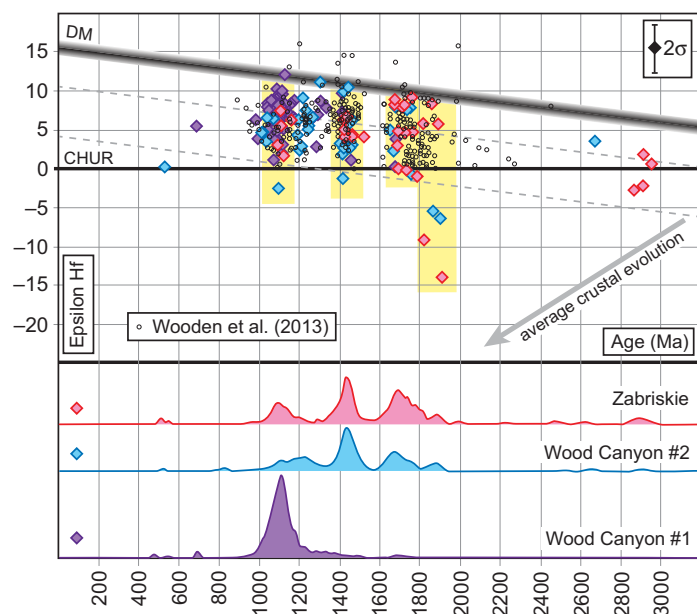
Figure 9. U-Pb and Hf data and interpretations for samples from southern California. Analyses are from the Neoproterozoic to Lower Cambrian Wood Canyon Formation (n = 204 for #1 and n = 197 for #2) and the Lower Cambrian Zabriskie Quartzite (n = 205). Diagrams and symbols are as in Figure 5.

Cambrian strata in eastern Alaska yield 1.8–1.3 Ga ages that are lacking in strata of British Columbia and from igneous rocks in the Wopmay orogen (Ross, 1991, 2002; Whitmeyer and Karlstrom, 2007; Fig. 1). Similar ages occur, however, in nearby Mesoproterozoic and Neoproterozoic sedimentary assemblages (Furlanetto et al., 2009; L. Lane, 2013, personal commun.), some Cambrian strata that accumulated along the northern Canadian passive margin (Hadlari et al., 2012), a broad range of circum-Arctic strata (Amato et al., 2009; Miller et al., 2006, 2010), and the Franklinian clastic wedge (Beranek et al., 2010; Anfinson et al., 2011) (Fig. 11). Our preferred interpretation is that these 1.8–1.3 Ga grains were shed from an as-yet-uncertain Precambrian basement province located along or outboard of Laurentia's Arctic margin (Fig. 13B).

Ordovician Time

Ordovician paleogeography became more complex with the onset of Caledonian tectonism along Laurentia's northeastern margin (McKerrow et al., 2000). Sea level was generally high, with Ordovician marine strata blanketing much of Laurentia (Sloss, 1988; Haq and Schutter, 2008).

Ordovician strata record a dramatic change in provenance (Ketner, 1968), with strata all along the Cordilleran margin dominated by >1.8 Ga grains (Fig. 16; Gehrels et al., 1995). The Peace River Arch (Figs. 1 and 13C) was a likely source given that it was emergent during this time, and also contains rocks of the appropriate age to have sourced relatively uncommon 2.1–2.0 Ga grains. The presence of 1.2–1.0 Ga grains with highly variable εHf$_{(t)}$ values suggests that some sediment may have been shed from northeastern Laurentia, where Grenville-age igneous rocks are in proximity to Archean crustal provinces (Hoffman, 1989). This shift in provenance, with possible influx of detritus from northeastern Laurentia, coincides with a ca. 0.45 Ga shift in provenance recorded by Nd isotopes, which is attributed by Patchett et al. (1999) to the onset of Caledonian-Appalachian tectonism.

These unique U-Pb age and Hf isotope characteristics are also found in off-shelf Ordovician strata in Nevada and Sonora, which is interpreted to link the off-shelf assemblages with the northern Cordilleran margin (cf. Wright and Wyld, 2006). Mississippian–Pennsylvanian strata in Nevada yield similar ages and Hf isotope characteristics, which is consistent with recycling from off-shelf assemblages that were emplaced onto the Cordilleran margin during the Devono-Mississippian Antler orogeny (Burchfiel et al., 1992; Gehrels and Dickinson, 2000).

Southward transport of sediment on the continental shelf during Ordovician time likely occurred due to longshore transport (Ketner, 1968, 1986; Gehrels et al., 1995). The occur-

rence of off-shelf assemblages with similar age and Hf isotope characteristics cannot be explained by simple westward spilling of sediment into deeper-water settings because the off-shelf sandstones are less mature and coarser grained than their on-shelf counterparts (Ketner, 1968). Possible explanations include: (1) transport of sediment southward along the margin in deep-water settings, perhaps in a trench (Gehrels et al., 1995, 2000b); (2) southward transport of the off-shelf assemblages by tectonic processes, e.g., sinistral transform faults (Wallin et al., 2000; Colpron and Nelson, 2009); (3) derivation from basement rocks exposed outboard of the Cordilleran margin (Ketner, 1968); and (4) derivation from regions other than western Laurentia, for example southeast Laurentia (Wright and Wyld, 2006).

One of the important constraints in considering these models is that the Vinini Formation, which is part of the off-shelf assemblage in Nevada, is dominated by grains that indicate derivation from the nearby Yavapai-Mazatzal and 1.48–1.34 Ga igneous provinces (Fig. 8). This would favor sedimentary transport models (1 and 3 above) rather than tectonic transport models (2 and 4), although proponents of tectonic transport (e.g., Wright and Wyld, 2006) raise the possibility that the Vinini Formation is in tectonic (rather than sedimentary) contact with other members of the off-shelf assemblage.

Devonian Time

Two major changes in provenance are recorded along the Cordilleran margin during mid-Paleozoic time (Figs. 13D, 17). The first is indicated by a return to U-Pb ages and εHf$_{(t)}$ values that suggest ultimate derivation from nearby basement provinces (with likely recycling through underlying Cambrian and Neoproterozoic strata) (yellow arrows on Fig. 13D). This change is recorded in Lower and Middle Devonian strata in northern British Columbia, Nevada, and Sonora.

A second change is recorded in Upper Devonian strata from eastern Alaska and southern British Columbia (red arrows on Fig. 13D), which record the influx of 0.70–0.40 Ga grains (Fig. 17) derived from circum-Laurentian magmatic and orogenic belts (e.g., Franklinian, Caledonian, Appalachian orogens; Fig. 1). Hf data for the young grains in eastern Alaska are quite distinctive, with juvenile to intermediate values that overlap εHf$_{(t)}$ values from the Franklinian clastic wedge (Anfinson et al., 2011). The Hf data also overlap with εHf$_{(t)}$ values from juvenile igneous rocks (Cecil et al., 2011) and detrital zircon grains (C. Tochilin, 2013, personal commun.) of the Alexander terrane, which may
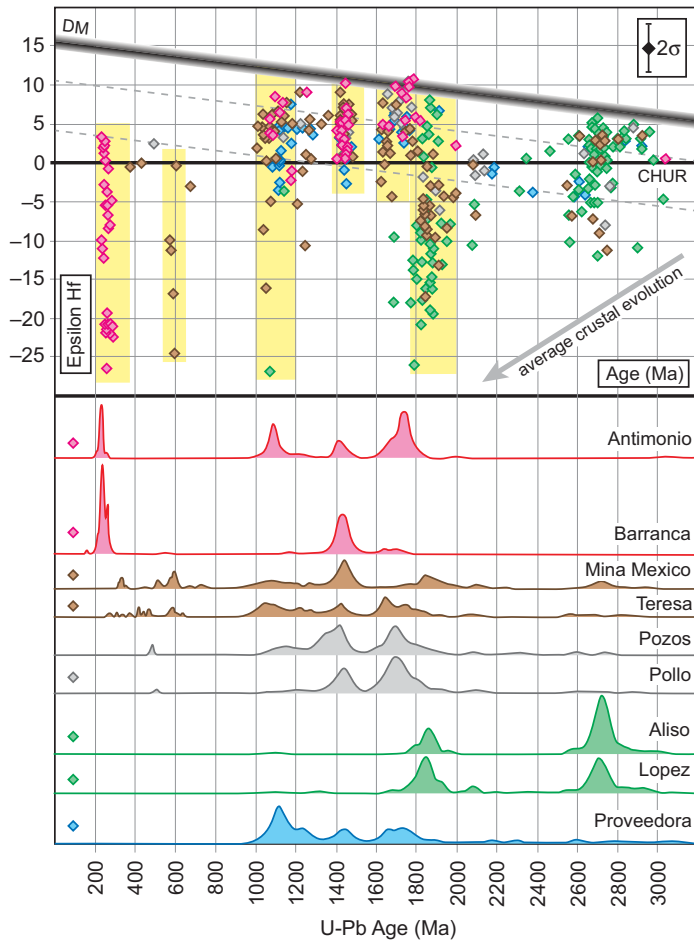
Figure 10. U-Pb and Hf data and interpretations for samples from Sonora. Analyses are from the Lower Cambrian Proveedora Quartzite (n = 145), Middle or Upper Ordovician Quartzite of Sierra Lopez (n = 190), Middle Ordovician Quartzite of Sierra El Aliso (n = 102), Upper Devonian Quartzite of Cerro Pollo (n = 198), Upper Devonian Los Pozos Formation (n = 90), Lower Permian Quartzite of Sierra Santa Teresa (n = 203), Lower Permian strata of the Mina Mexico Formation (n = 205), Upper Triassic Barranca Group (n = 205), and Upper Triassic Antimonio Formation (n = 102). Note that the relative height of the young age peak in Barranca Group has been reduced by a factor of 2×. Diagrams and symbols are as in Figure 5.
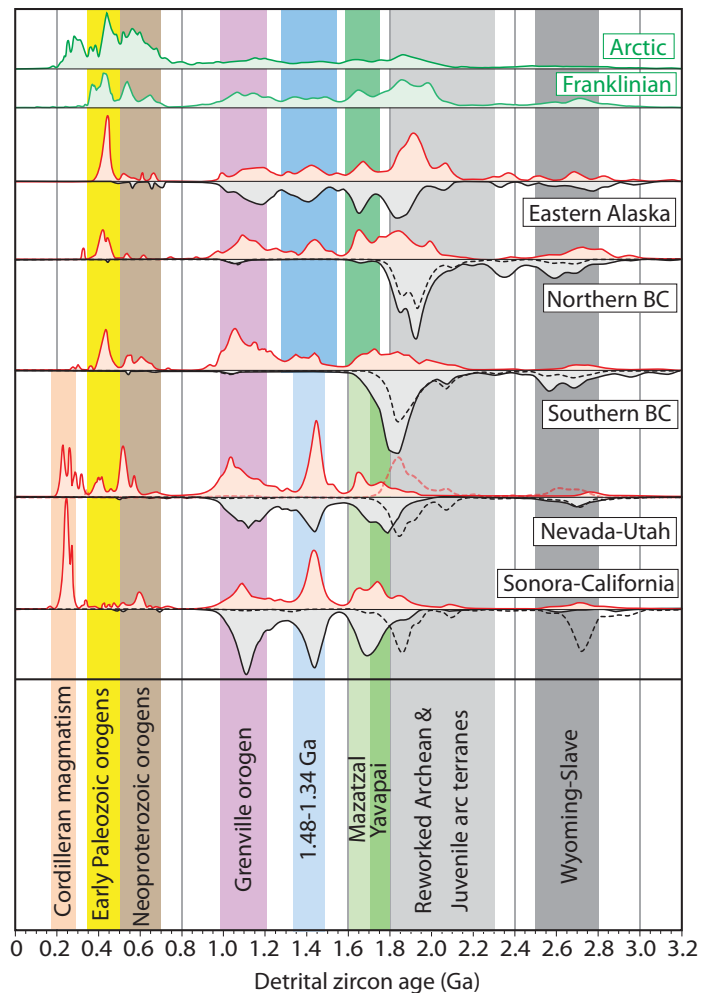
Figure 11. Probability density plots of U-Pb ages from each transect, shown relative to general age ranges of basement provinces in North America (vertical shaded bands; Hoffman, 1989; Whitmeyer and Karlstrom, 2007). Ages from Neoproterozoic, Cambrian, and Lower–Middle Devonian strata are shown with gray shading; ages from most Upper Devonian through Permian and Triassic strata are shown with red shading. Dashed black lines represent ages from Ordovician strata. Dashed red line for Nevada-Utah represents ages from Mississippian–Pennsylvanian strata interpreted to have been derived from the Antler highlands. Green reference curves include ages from Paleozoic strata of the Franklinian orogen (Beranek et al., 2010; Anfinson et al., 2011) and from strata in the Arctic (Seward Peninsula data of Amato et al., 2009; Wrangel Island data of Miller et al., 2010; and circum-Arctic Triassic strata of Miller et al., 2006). BC—British Columbia.

have been located along the paleo-Arctic margin during Devonian time (Soja, 1994; Gehrels et al., 1996; Colpron and Nelson, 2007, 2009).

Similar changes in provenance are also recorded by U-Pb ages from strata along the Arctic and northern Cordilleran margins (Beranek et al., 2010; Lemieux et al., 2011), with 0.70–0.40 Ga grains appearing in Middle Devonian strata and becoming dominant in Upper Devonian through Mississippian strata. A similar shift is also recorded in Paleozoic strata of the Grand Canyon in southwestern North America, where <0.70 Ga grains first appear in Middle and Upper Devonian conglomeratic strata of the Temple Butte Formation (Gehrels et al., 2011).

Mississippian-Pennsylvanian-Permian Time

Provenance patterns during Mississippian–Permian time are complex due to orogenic activity along all margins of Laurentia, evolving paleogeographic patterns within Laurentia due to uplift of the Ancestral Rocky Mountains
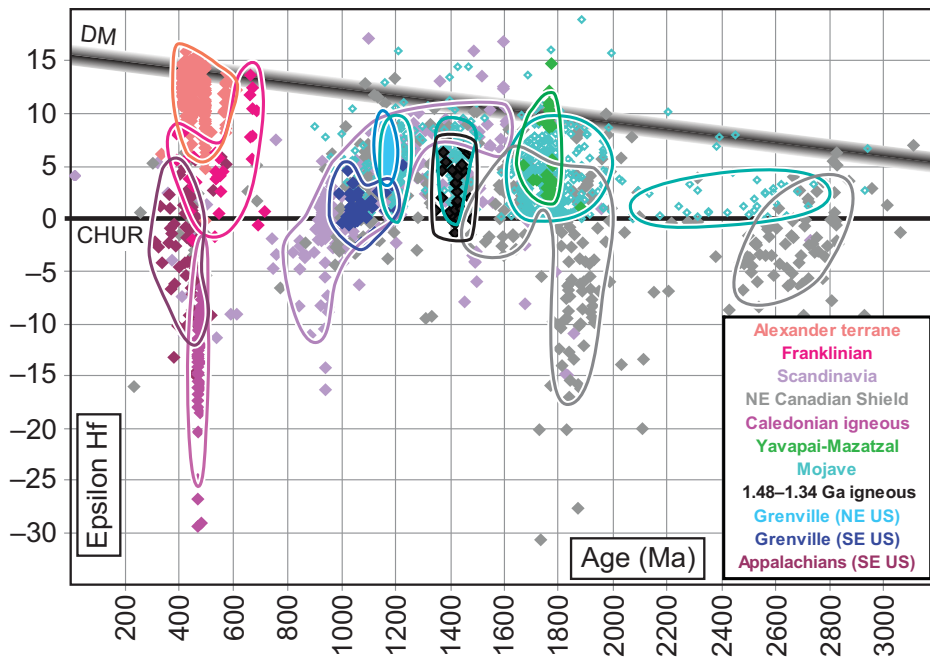
Figure 12. Relevant Hf isotope data available for Laurentia and Scandinavia, shown as individual analyses and approximate encircling fields. Data sets are as follows: Alexander terrane—early Paleozoic plutonic rocks (Cecil et al., 2011) and detrital zircons from Paleozoic and Triassic strata (C. Tochilin, 2013, personal commun.); Franklinian—detrital zircons from Neoproterozoic to Upper Devonian strata of the Franklinian foreland basin in the Canadian Arctic Islands (Anfinson et al., 2012); Scandinavia—Paleoproterozoic and Mesoproterozoic igneous rocks of Norway and Sweden (Andersen and Griffin, 2004; Andersen et al., 2002, 2007; Andersson et al., 2011; Brander et al., 2011), and detrital zircons in Permian strata of the Oslo Rift (Andersen et al., 2011); NE Canadian Shield—detrital zircons in Cretaceous strata of the Sverdrup Basin (Rohr et al., 2010) and the Wandel Sea Basin (Rohr et al., 2008); Caledonian igneous—Ordovician granites in Scotland (Appleby et al., 2010) and Ireland (Flowerdew et al., 2009); Yavapai-Mazatzal—Paleoproterozoic igneous rocks in Colorado (Bickford et al., 2008); Mojave—Paleoproterozoic and Mesoproterozoic igneous rocks and detrital zircons in Neoproterozoic and Cambrian strata in the Mojave province of southern California (Wooden et al., 2013); 1.48–1.34 Ga igneous—1.48–1.34 Ga granitoids of the U.S. midcontinent region (Goodge and Vervoort, 2006); Grenville (NE U.S.)—Mesoproterozoic plutonic rocks of the Adirondack Mountains, northeastern U.S. (Bickford et al., 2010); Grenville (SE U.S.) —>0.95 Ga detrital zircons in a modern river in the southern Appalachian Mountains, southeast U.S. (Mueller et al., 2008); Appalachians (SE U.S.)—<0.95 Ga detrital zircons in a modern river in the southern Appalachian Mountains, southeast U.S. (Mueller et al., 2008). DM—depleted mantle; CHUR—chondritic uniform reservoir.

(Kluth and Coney, 1981; Fig. 13E), and likely recycling of detritus from Devonian and older units (Fig. 18).

Our data from Permian units in Sonora record the presence of several different source regions. Most obvious are 1.8–1.6 Ga and 1.48–1.34 Ga grains that yield ages and Hf isotope signatures similar to the Mojave-Yavapai-Mazatzal and 1.48–1.34 Ga igneous provinces, suggesting ultimate derivation from local basement rocks. These units also have abundant 1.2–1.0 Ga grains that could have been shed directly from the Grenville orogen, or perhaps recycled from

underlying Devonian and older units. Archean grains and 2.0–1.8 Ga grains with intermediate to evolved $\varepsilon Hf_{(t)}$ values are also abundant. These old components could have been recycled from Ordovician strata or shed from older components within the local basement (e.g., Bickford et al., 2008; Shufeldt et al., 2010; Wooden et al., 2013). Yet another source is recorded by ca. 0.60 Ga grains with moderately to highly evolved $\varepsilon Hf_{(t)}$ values. These grains were presumably shed from an outboard source given the scarcity of ca. 0.60 Ga igneous rocks emplaced into Precambrian basement in southwestern North America.

Finally, two ca. 0.40 Ga grains with intermediate $\varepsilon Hf_{(t)}$ values may have been shed from the Appalachian orogen, as has been suggested for coeval strata in the Grand Canyon (Gehrels et al., 2011).

As described above, Mississippian and Pennsylvanian strata in Nevada were derived from the Antler highlands to the west. This expression of circum-Laurentia tectonism is similar in timing with the other changes noted, but the presence of mainly >1.8 Ga grains in upper Paleozoic strata of Nevada-Utah is quite different from the occurrence of Neoproterozoic–Paleozoic grains in other regions.

Our Pennsylvanian sample from southern British Columbia (Spray Lakes Group) records several different source regions. The dominant grains with ages between 2.0 and 1.0 Ga have a range of juvenile to evolved $\varepsilon Hf_{(t)}$ values that are somewhat more evolved than most data from the Yavapai-Mazatzal and 1.48–1.34 Ga provinces to the south. This suggests that they may have been shed from the enigmatic northwestern Laurentian basement province noted above. Grains of 0.60–0.40 Ga were apparently shed from two different source regions, one with more evolved compositions (perhaps the Caledonides) and a second comprising more juvenile crust (perhaps juvenile arc terranes in the Arctic basin) (Fig. 18).

Triassic Time

In Nevada-Utah, sedimentary provenance has been reconstructed in considerable detail by U-Pb geochronologic analysis of many Triassic samples (Riggs et al., 1996, 2012; Dickinson and Gehrels, 2008). The main conclusion from these studies is that Triassic sandstones of the southwest were derived largely from local basement rocks, the Ouachita-Marathon orogenic system along the southern Laurentian margin, and Permo-Triassic igneous rocks that formed in Cordilleran magmatic arcs.

Our U-Pb and Hf data generally support these provenance interpretations (Fig. 13F). For Nevada-Utah, derivation of zircons from basement rocks of the southwest U.S. is indicated by Hf data that overlap with summary fields for the Yavapai-Mazatzal and 1.48–1.34 Ga provinces (Fig. 19). Grains of 1.2–1.0 Ga and 0.60–0.40 Ga age may have been shed from the Ouachita-Marathon orogen. The large range of $\varepsilon Hf_{(t)}$ values for 0.30–0.20 Ga grains suggests that these Cordilleran-margin arcs consist largely of relatively juvenile Yavapai-Mazatzal and 1.48–1.34 Ga crust as well as crust of Archean heritage. The presence of such old crustal components in the southwest has previously been recognized in Precambrian basement of Colorado (Bickford et al., 2008),
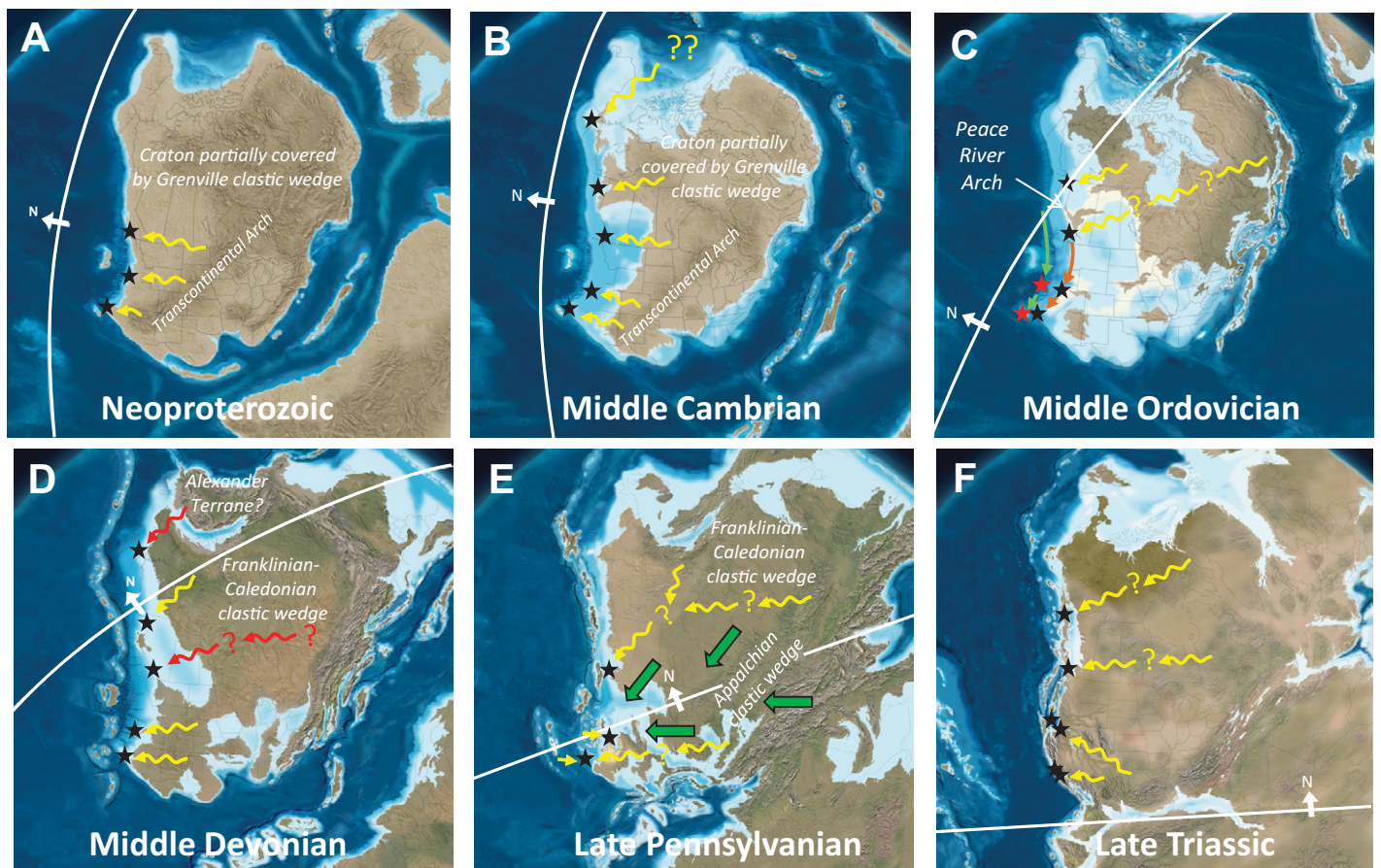
Figure 13. Paleogeographic maps of Laurentia from Neoproterozoic through Triassic time (from Ron Blakey, http://jan.ucc.nau.edu/rcb7 /nam.html). Stars represent approximate positions of samples; white lines show approximate positions of paleo-equator. (A) Neoproterozoic time. Provenance is mainly from basement rocks exposed nearby and along the flanks of the Transcontinental Arch, with at least local reworking of Grenville-derived clastic strata. (B) Cambrian time. Derivation of most sediment is from nearby basement rocks and from the flanks of the Transcontinental Arch in southern and central Laurentia. Eastern Alaska records derivation from an uncertain landmass, perhaps located along the northern Laurentian margin. (C) Ordovician time. Interpreted provenance of most detritus is from the Peace River Arch region of the northern Canadian Shield, with possible input from northeastern portions of the shield. (D) Devonian time. Derivation is from local basement sources (with possible recycling through underlying strata) during Early–Middle Devonian time (yellow arrows), with input from Franklinian-Caledonian sources beginning in Late Devonian time (red arrows). (E) Mississippian–Pennsylvanian time. Derivation is in part from local basement sources (with significant recycling), and also from influx of sediment from uplifted off-shelf assemblages to the west. There is possible transport from trade winds (shown schematically with green arrows). (F) Triassic time. Derivation is from both local and distant sources, with known river systems in the southwest (Dickinson and Gehrels, 2008) and hypothesized equivalents to the north.

northwestern Arizona (Shufeldt et al., 2010), and southern California (Wooden et al., 2013).

U-Pb and Hf data for zircons in Triassic strata of Sonora are quite similar to the values from Nevada-Utah, and provenance interpretations are accordingly similar. Significant differences are the lack of 0.6–0.4 Ga grains and the presence of 0.3–0.2 Ga grains with even more evolved $\varepsilon Hf_{(t)}$ values. A likely scenario is that these ancient crustal components are associated with the Mojave province (Wooden et al., 2013), offset from southern California along the Mojave-Sonora megashear during Mesozoic time (Anderson et al., 2005).

Triassic strata in the northern Cordillera contain abundant detritus from >1.8 Ga rocks of the Canadian Shield, little material from juvenile provinces to the south, abundant 1.2–1.0 Ga material ultimately derived from the Grenville province, and abundant 0.60–0.40 Ga grains with intermediate to slightly evolved Hf values (Fig. 19). The latter grains are more negative than would be expected from the Franklinian system to the north, but are consistent with derivation from the Caledonian-Appalachian system in eastern Laurentia. These grains may have been reworked from the Caledonian-Appalachian clastic wedge that blanketed northern Laurentia

during late Paleozoic time (Patchett et al., 1999), or perhaps carried across Laurentia in Triassic river and/or aeolian systems (Fig. 13F).

DETRITAL ZIRCON U-Pb AND Hf REFERENCE DATA

The U-Pb ages and $\varepsilon Hf_{(t)}$ values described above provide a relatively robust characterization of zircon grains that accumulated along the western Laurentian margin during Neoproterozoic through Triassic time. These data also help constrain the Hf characteristics and evolution of Laurentian basement provinces for which little
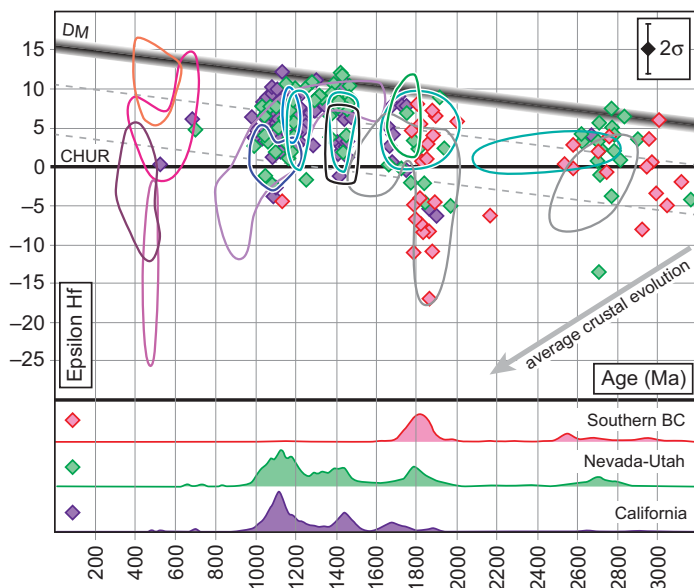
Figure 14. U-Pb and Hf isotope data from Neoproterozoic strata. Diagrams and symbols are defined in Figure 5; reference fields are defined in Figure 12. BC—British Columbia.
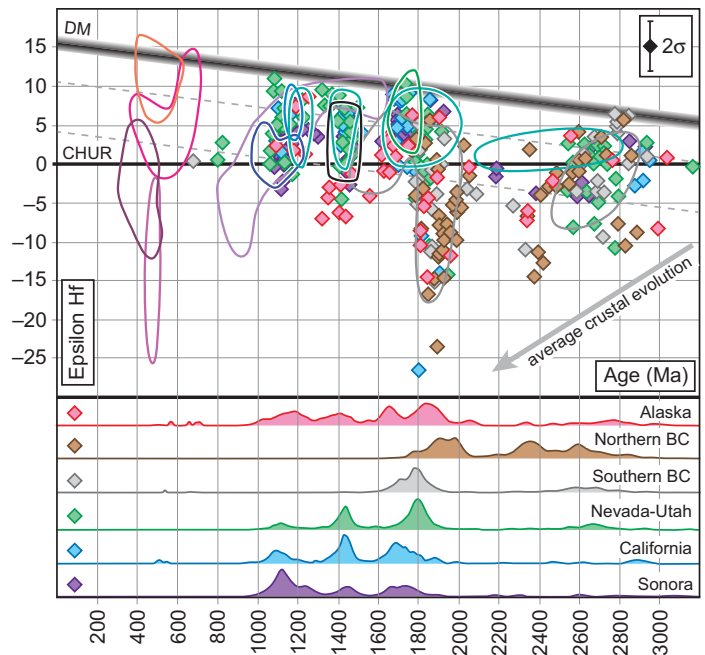

Figure 15. U-Pb and Hf isotope data from Cambrian strata. Diagrams and symbols are defined in Figure 5; reference fields are defined in Figure 12. BC—British Columbia.

or no Hf isotopic information is available. The main patterns in space and time are summarized below and in Figures 16, 20, and 21.

1. The U-Pb ages and Hf isotope compositions of detrital zircon grains in Neoproterozoic, Cambrian, and Lower–Middle Devonian strata vary considerably along strike (Fig. 20). Southern transects are dominated by three subequal age groups of 1.8–1.6, 1.48–1.34, and 1.2–1.0 Ga. εHf$_{(t)}$ values for these grains are juvenile to intermediate, with little evidence of incorporation of Archean crustal materials. Strata from southern and northern British Columbia yield major peaks between 2.0 and 1.7 Ga, a lesser age group at 2.8–2.5 Ga, and scattered ages between 2.5 and 2.0 Ga. The Hf data record significant influence of Archean crustal materials of the Canadian Shield, with mostly evolved and intermediate εHf$_{(t)}$ values in the dominant 1.84–1.78 Ga grains. Strata from Alaska yield dominantly Archean and Paleoproterozoic ages, and also have younger age peaks at 1.7–1.6, 1.45–1.35, and 1.25–1.0 Ga. εHf$_{(t)}$ values for these grains are generally more evolved than from coeval grains to the south (e.g., from the Yavapai-Mazatzal and 1.48–1.34 Ga igneous provinces), suggesting derivation from northern source regions containing more evolved crust.

2. Ordovician strata all along the Cordilleran margin yield mainly >1.78 Ga grains with U-Pb ages and Hf isotope compositions that are similar along strike (Fig. 16). This precludes the use

of Ordovician strata to reconstruct the latitudinal position of terranes along the margin. An additional complexity arises from the occurrence of similar ages and εHf$_{(t)}$ values in upper Paleozoic strata of Nevada-Utah and Sonora, which complicates the use of these strata for reconstructing paleolatitude.

3. Upper Paleozoic and Triassic strata generally yield >1.0 Ga zircon grains with ages and εHf$_{(t)}$ patterns that suggest ultimate derivation from relatively local bedrock sources (Fig. 21). These strata also have abundant <1.0 Ga grains, with main age groups of 0.70–0.35 Ga and, in southern transects, 0.30–0.22 Ga (Fig. 21). The Hf isotopic composition of 0.70–0.35 Ga grains changes along strike, with juvenile to intermediate values in Alaska, evolved compositions in British Columbia, and intermediate compositions in Nevada-Utah. This variation is interpreted to reflect the influence of juvenile magmatic arc systems (e.g., Alexander terrane) in Alaska, derivation from the Caledonides in British Columbia (e.g., Patchett et al., 1999), and derivation from the Appalachian orogen (and possibly the Ouachita-Marathon system) in Nevada-Utah and Sonora (e.g., Gehrels et al., 2011). Grains of 0.30–0.22 Ga in the southern transects have variable Hf isotope compositions that are interpreted to reflect the presence of Archean crustal components within Paleoproterozoic basement provinces of the southwest (Bickford et al., 2008; Shufeldt et al., 2010; Wooden et al., 2013).

COMPARISON WITH GLOBAL Hf DATA

An interesting view of our western North American Hf data is provided by comparison with global Hf data for detrital zircons (Fig. 22), as compiled by Belousova et al. (2010). The latter data set (gray crosses for individual analyses, black line for running average) consists of U-Pb and εHf$_{(t)}$ values determined on 13,844 zircons recovered mainly from modern rivers in Australia, Asia, and South America, with lesser contributions from North America, Africa, and Antarctica.

Western North America records a somewhat different Precambrian magmatic history from the global average, with greater proportions of 2.0–1.8, 1.5–1.4, and 1.2–1.0 Ga grains, and reduced proportions of 2.3–2.0, 1.7–1.5, and 0.9–0.7 Ga grains (Fig. 22). The Hf data show even greater differences, with North American zircons recording greater proportions of juvenile magmatism during Archean (3.0–2.5 Ga), late Paleoproterozoic–Mesoproterozoic (1.8–1.0 Ga), and Neoproterozoic–early Paleozoic (0.7–0.4 Ga) time, and greater degrees of interaction with Archean crust during Paleoproterozoic (2.2–1.8 Ga) and late Paleozoic–early Mesozoic (0.30–0.22 Ga) time. The overall greater abundance of juvenile crust in western North America may be due to the concentration of juvenile terranes by transform tectonics (e.g., Patchett and Chase, 2002).
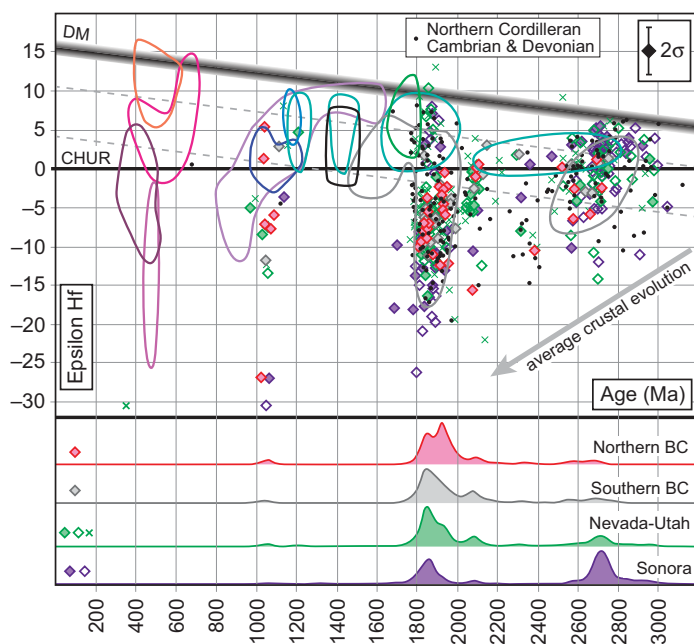
Figure 16. U-Pb and Hf isotope data from Ordovician strata, and from northern Cordilleran strata of Cambrian and Devonian age. Diagrams and symbols are defined in Figure 5; reference fields are defined in Figure 12. BC—British Columbia.
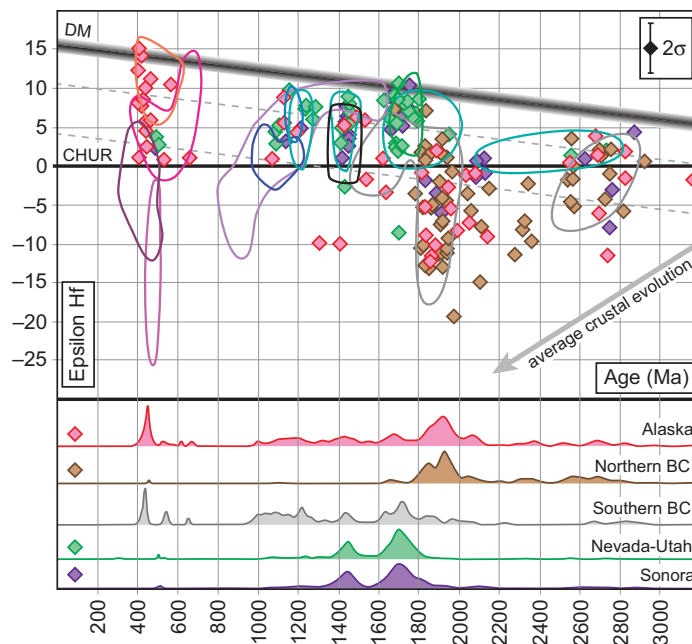
Figure 17. U-Pb and Hf isotope data from Devonian strata. Diagrams and symbols are defined in Figure 5; reference fields are defined in Figure 12. BC—British Columbia.

Although our western North American data differ from the global data set as noted above, the overall patterns of crustal growth versus reworking inferred from our data are highly compatible with the global patterns reported by Condie et al. (2011), Belousova et al. (2010), Hawkesworth et al. (2010), Roberts (2012), and Cawood et al. (2012). These first-order patterns include (1) significant juvenile crustal growth during Archean (3.2–2.6 Ga) time, (2) profound reworking of Archean crust during Paleoproterozoic (2.0–1.8 Ga) assembly of the Nuna/Columbia supercontinent, (3) renewed growth of juvenile crust, presumably by plate tectonic processes operating in an oceanic accretionary orogen, between 1.78 and 1.2 Ga, (4) reworking mainly of this 1.78–1.2 Ga crust during 1.2–1.0 Ga assembly of the Rodinia supercontinent, and (5) processes of Phanerozoic crustal growth and recycling that are globally variable depending on local tectonic settings and the availability of ancient crustal materials.

CONCLUSIONS

U-Pb geochronology and Hf isotope geochemistry of detrital zircons from sandstones of the Cordilleran margin yield four primary contributions to understanding the sediment dispersal patterns and crustal evolution of western North America.

First is the generation of a robust reference for the ages and Hf isotopic compositions of detrital zircon grains that accumulated along Laurentia's western margin during Cambrian (locally Neoproterozoic) through Triassic time (Figs. 16, 20, 21). This reference is useful for comparison with inboard sandstones that accumulated on the North American craton and with outboard strata in potentially displaced Cordilleran terranes.

Second is enhanced characterization of the age and Hf isotopic composition of western Laurentian basement provinces and magmatic assemblages (Figs. 20 and 21). In southern transects, abundant 1.8–1.3 Ga grains with juvenile to intermediate $\varepsilon Hf_{(t)}$ values provide an excellent reference for the Hf isotopic composition of the Mojave, Yavapai, Mazatzal, and 1.48–1.34 igneous provinces, complementing the Hf data available from igneous rocks (Goodge and Vervoort, 2006; Bickford et al., 2008; Wooden et al., 2013). The presence of abundant >1.8 Ga grains and evolved $\varepsilon Hf_{(t)}$ values in <1.0 Ga grains also demonstrates the existence of older crustal components in the southwest (e.g., Bickford et al., 2008; Shufeldt et al., 2010; Wooden et al., 2013). In northern transects, abundant >2.5 Ga and 2.0–1.8 Ga grains yield a rich record of the ages and Hf isotope compositions of the western Canadian Shield (Figs. 20 and 21). Some grains were also shed from as-yet-unrecognized

1.7–1.3 Ga basement rocks that may be located in northwestern Laurentia or elsewhere within the Arctic realm.

Third are better constraints on the provenance of Cordilleran passive-margin sandstones, which yield new insights into connections between sediment dispersal and changes in tectonism, paleogeography, and sea level. First-order provenance patterns are as follows:

(1) Neoproterozoic and Cambrian strata were derived mainly from nearby basement rocks, with addition of 1.2–1.0 Ga grains recycled from the Mesoproterozoic Grenville clastic wedge. This relatively simple provenance pattern reflects Neoproterozoic emergence of the Transcontinental Arch in the continental interior and accumulation of passive-margin sequences along Laurentia's rifted margins (Figs. 13A, 13B).

(2) Ordovician strata all along the Cordilleran margin record derivation from the northern Canadian Shield, with sediment carried southward in on-shelf settings by longshore currents and in off-shelf environments by either bathymetrically channeled submarine fans or coastwise tectonic transport. This unusual provenance pattern is interpreted to have resulted mainly from high sea level during Ordovician time, perhaps leaving the northwestern Canadian Shield (specifically the Peace River Arch) as the only emergent region along the Cordilleran margin (Fig. 13C).
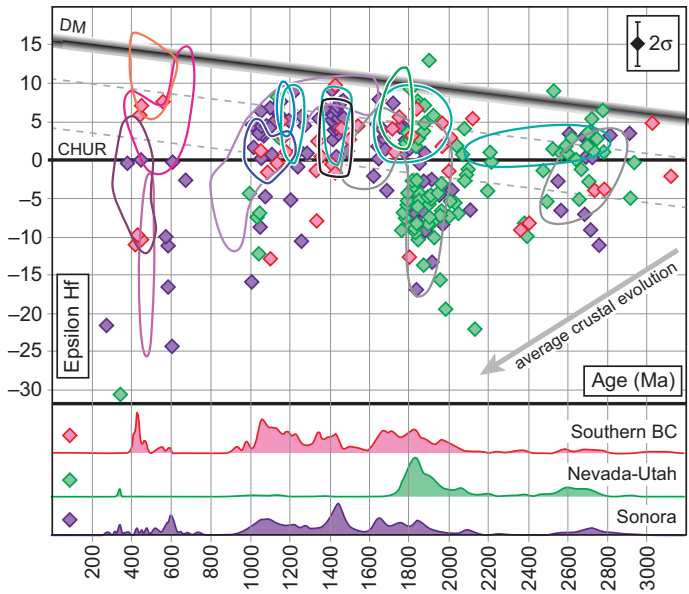
Figure 18. U-Pb and Hf isotope data from Mississippian, Pennsylvanian, and Permian strata. Diagrams and symbols are defined in Figure 5; reference fields are defined in Figure 12. BC—British Columbia.
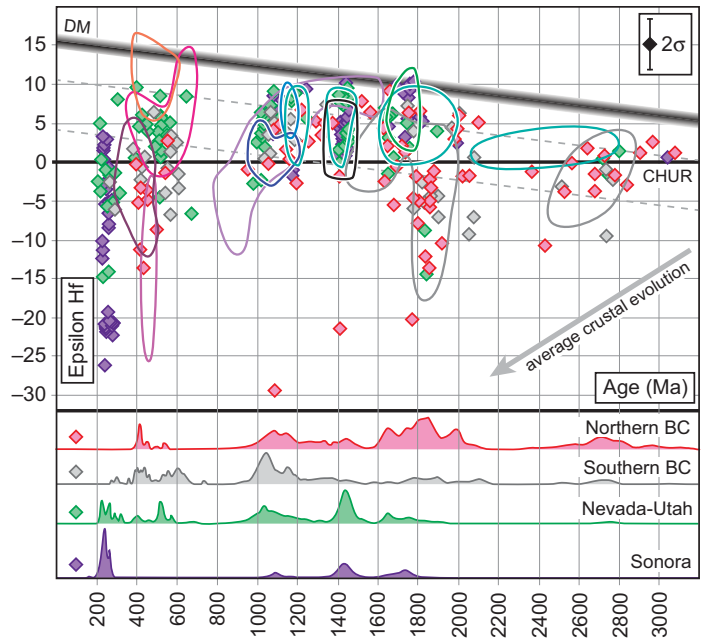

Figure 19. U-Pb and Hf isotope data from Triassic strata. Diagrams and symbols are defined in Figure 5; reference fields are defined in Figure 12. BC—British Columbia.
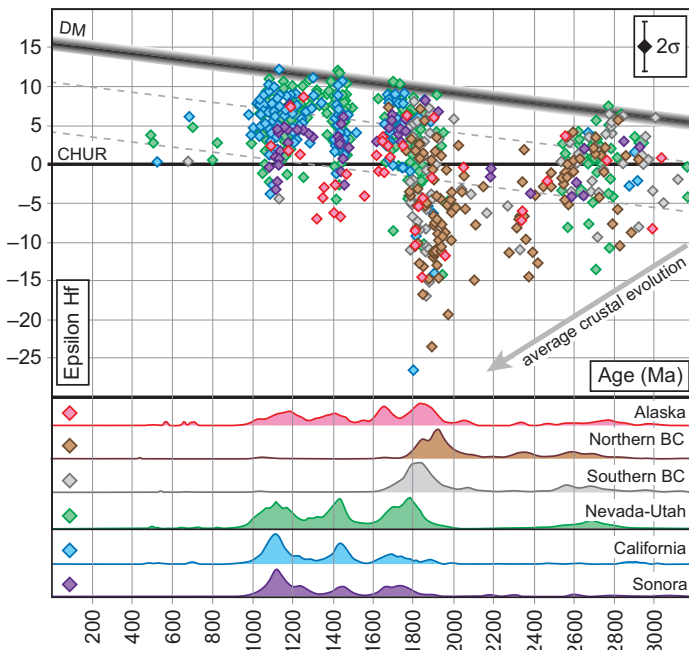

Figure 20. Summary of U-Pb and Hf isotopic data for grains in Neoproterozoic, Cambrian, and Lower or Middle Devonian strata from each transect. Diagrams and symbols are defined in Figure 5. BC—British Columbia.
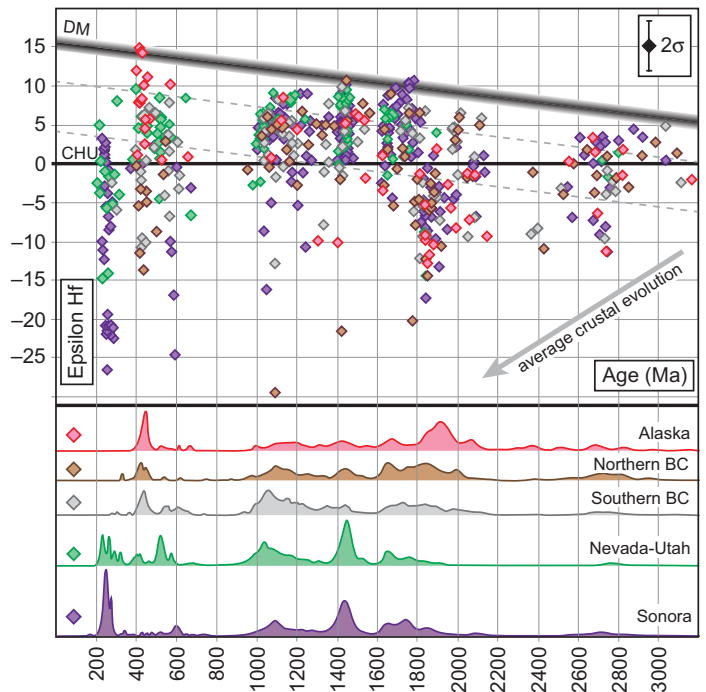

Figure 21. Summary of U-Pb and Hf isotopic data for grains in Upper Devonian, Mississippian, Pennsylvanian, Permian, and Triassic strata from each transect. Diagrams and symbols are defined in Figure 5. BC—British Columbia.
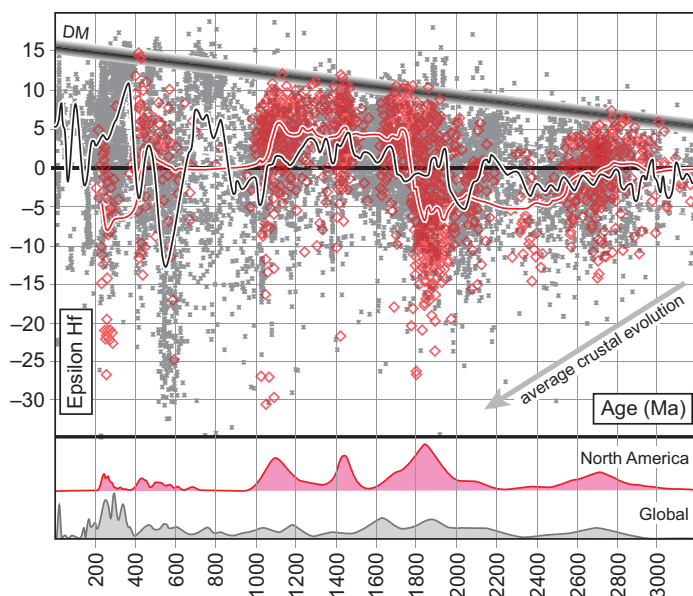
Figure 22. Comparison of all data from this study (red symbols) with Hf isotope information from modern rivers around the world (gray symbols; from compilation of Belousova et al., 2010). Black curve shows the running average of global detrital zircon data. Red curve shows the running average of western Laurentia data. Gray probability density plot (PDP) is the summary of all U-Pb ages from the global database; red PDP is the summary of western Laurentian ages. DM—depleted mantle.

REFERENCES CITED

Amato, J.M., Toro, J., Miller, E.L., Gehrels, G.E., Farmer, G.L., Gottlieb, E.S., and Till, A.B., 2009, Late Proterozoic–Paleozoic evolution of the Arctic Alaska–Chukotka terrane based on U-Pb igneous and detrital zircon ages: Implications for Neoproterozoic paleogeographic reconstructions: Geological Society of America Bulletin, v. 121, p. 1219–1235, doi:10 1130/B26510.1.

Amelin, Y., Lee, D.-C., Halliday, A.N., and Pidgeon, R.T., 1999, Nature of the Earth's earliest crust from hafnium isotopes in single detrital grains: Nature, v. 399, p. 252–255, doi:10.1038/20426.

Andersen, T., and Griffin, W.L., 2004, Lu-Hf and U-Pb isotope systematics of zircons from the Storangen intrusion, Rogaland Complex, SW Norway: Implications for the composition and evolution of Precambrian lower crust in the Baltic Shield: Lithos, v. 73, p. 271–288, doi:10.1016/j.lithos.2003.12.010.

Andersen, T., Griffin, W.L., and Pearson, N.J., 2002, Crustal evolution in the SW part of the Baltic Shield: The Hf isotope evidence: Journal of Petrology, v. 43, p. 1725–1747, doi:10.1093/petrology/43.9.1725.

Andersen, T., Griffin, W.L., and Sylvester, A.G., 2007, Sveconorwegian crustal underplating in southwestern Fennoscandia: LAM-ICPMS U-Pb and Lu-Hf isotope evidence from granites and gneisses in Telemark, southern Norway: Lithos, v. 93, p. 273–287, doi: 10.1016/j.lithos.2006.03.068.

Andersen, T., Saeed, A., Gabrielsen, R.H., and Olaussen, S., 2011, Provenance characteristics of the Brumunddal sandstone in the Oslo Rift derived from U-Pb, Lu-Hf and trace element analyses of detrital zircons by laser ablation ICMPS: Norwegian Journal of Geology, v. 91, p. 1–19.

Anderson, T.H., Nourse, J.A., McKee, J.W., and Steiner, M.B., eds., 2005, The Mojave-Sonora Megashear Hypothesis: Development, Assessment, and Alternatives: Boulder, Colorado, Geological Society of America, Special Paper 393, 693 p.

Andersson, U.B., Begg, G.C., Griffin, W.L., and Högdahl, K., 2011, Ancient and juvenile components in the continental crust and mantle: Hf isotopes in zircon from Svecofennian magmatic rocks and rapakivi granites in Sweden: Lithosphere, v. 3, p. 409–419, doi:10.1130 /L162.1.

Anfinson, O.A., Leier, A.L., Embry, A.F., and Dewing, K., 2011, Detrital zircon geochronology and provenance of the Neoproterozoic to Late Devonian Franklinian Basin, Canadian Arctic Islands: Geological Society of America Bulletin, v. 124, p. 415–430, doi:10.1130 /B30503.1.

Anfinson, O.A., Leier, A.L., Gaschnig, R., Embry, A.F., and Dewing, K., 2012, U–Pb and Hf isotopic data from Franklinian Basin strata: Insights into the nature of Crockerland and the timing of accretion, Canadian Arctic Islands: Canadian Journal of Earth Sciences, v. 49, p. 1316–1328, doi:10.1139/e2012-067.

Appleby, S.K., Gillespie, M.R., Graham, C.M., Hinton, R.W., Oliver, G.J.H., and Kelly, N.M., 2010, Do S-type

(3) Lower and Middle Devonian strata record a return to relatively local derivation of sediment, with considerable recycling of detrital zircons from underlying pre-Ordovician strata, presumably due to re-emergence of nearby basement and cover strata (Fig. 13D).

(4) Upper Devonian, Mississippian, Pennsylvanian, and Permian strata record local derivation (with considerable recycling) as well as a major influx of 0.70–0.40 Ga grains derived from circum-Laurentian orogenic systems (Fig. 13D, 13E). Hf isotope compositions of these young grains reflect contributions, from north to south, from mainly juvenile arc terranes along the Arctic/Franklinian margin, highly evolved igneous rocks in the Caledonides, moderately evolved igneous rocks in the Appalachians, and possibly more juvenile peri-Gondwana sources in the Ouachita-Marathon orogen. Orogenic activity is also recorded along the southern Cordilleran margin by an influx of >1.8 Ga grains derived from off-shelf Ordovician assemblages exposed in the Antler highlands (and equivalent features along strike).

(5) Triassic strata have contributions from local sources, grains ultimately derived from distant Laurentian-margin orogenic systems, and, in southern transects, grains derived from

Permo-Triassic magmatic arcs built along the southern Cordilleran margin (Fig. 13F).

Fourth is a refined understanding of the growth and evolution of western North American crust (Figs. 20 and 21). Our new data, together with existing geochemical and isotopic information (summarized by Whitmeyer and Karlstrom, 2007), record a chronology of major crustal growth during late Archean (>2.6 Ga) time; dramatic reworking of this crust and generation of little or no juvenile crust between 2.0 and 1.78 Ga; generation of significant volumes of juvenile crust between 1.78 and 1.6 Ga; reworking of this juvenile crust, with moderate generation of new crust, at 1.48–1.34 and 1.2–1.0 Ga; reworking of mainly Mesoproterozoic crust and generation of new crust at 0.70–0.40 Ga; and mostly reworking of older crust in Permo-Triassic magmatic arcs along the southern Cordilleran margin.

In comparison with global Hf data (Fig. 22), western North America records a somewhat different record of crustal genesis and reworking, with greater amounts of juvenile crust during Archean time and between 1.80 and 0.40 Ga, and a greater degree of reworking of ancient crust between 2.2 and 1.8 Ga and 0.30–0.22 Ga.

granites commonly sample infracrustal sources? New results from an integrated O, U–Pb and Hf isotope study of zircon: Contributions to Mineralogy and Petrology, v. 160, p. 115–132, doi:10.1007/s00410-009-0469-3.

Bahlburg, H., Vervoort, J.D., DuFrane, S.A., Bock, B., Augustsson, C., and Reimann, C., 2009, Timing of crust formation and recycling in accretionary orogens: Insights learned from the western margin of South America: Earth-Science Reviews, v. 97, p. 215–241.

Bahlburg, H., Vervoort, J.D., DuFrane, S.A., Carlotto, V., Reimann, C., and Cardenas, J., 2011, The U–Pb and Hf isotope evidence of detrital zircons of the Ordovician Ollantaytambo Formation, southern Peru, and the Ordovician provenance and paleogeography of southern Peru and northern Bolivia: Journal of South American Earth Sciences, v. 32, p. 196–209, doi:10.1016/j.jsames.2011.07.002.

Belousova, E.A., Kostitsyn, Y.A., Griffin, W.L., Begg, G.C., O'Reilly, S.Y., and Pearson, N.J., 2010, The growth of continental crust: Constraints from zircon Hf-isotope data: Lithos, v. 119, p. 457–466, doi:10.1016/j.lithos.2010.07.024.

Beranek, L.P., Mortensen, J.K., Lane, L.S., Allen, T.L., Fraser, T.A., Hadlari, T., and Zantvoort, W.G., 2010, Detrital zircon geochronology of the western Ellesmerian clastic wedge, northwestern Canada: Insights on Arctic tectonics and the evolution of the northern Cordilleran miogeocline: Geological Society of America Bulletin, v. 122, p. 1899–1911, doi:10.1130/B30120.1.

Bickford, M.E., Mueller, P.A., Kamenov, G.D., and Hill, B.M., 2008, Crustal evolution of southern Laurentia during the Paleoproterozoic: Insights from zircon isotopic studies of ca. 1.75 Ga rocks in central Colorado: Geology, v. 36, p. 555–558, doi:10.1130/G24700A.1.

Bickford, M.E., McLelland, J.M., Mueller, P.A., Kamenov, G.D., and Neadle, M., 2010, Hafnium isotopic compositions of zircon from Adirondack AMCG suites: Implications for the petrogenesis of anorthosites, gabbros, and granitic members of the suites: Canadian Mineralogist, v. 48, p. 751–761, doi:10.3749/canmin.48.2.751.

Bouvier, A., Vervoort, J.D., and Patchett, J.D., 2008, The Lu-Hf and Sm-Nd isotopic composition of CHUR: Constraints from unequilibrated chondrites and implications for the bulk composition of terrestrial planets: Earth and Planetary Science Letters, v. 273, p. 48–57, doi:10.1016/j.epsl.2008.06.010.

Brander, L., Soderlund, U., and Bingen, B., 2011, Tracing the 1271–1246 Ma Central Scandinavian dolerite group mafic magmatism in Fennoscandia: U-Pb baddeleyite and Hf isotope data on the Moslatt and Borgefjell dolerites: Geological Magazine, v. 148, p. 632–643, doi:10.1017/S0016756811000033.

Burchfiel, B.C., Cowan, D.S., and Davis, G.A., 1992, Tectonic overview of the Cordilleran orogen in the western United States, *in* Burchfiel, B.C., Lipman, P.W., and Zoback, M.L., eds., The Cordilleran Orogen: Conterminous U.S.: Boulder, Colorado, Geological Society of America, The Geology of North America, v. G-3, p. 407–480.

Cawood, P.A., Hawkesworth, C.J., Dhuime, B., 2012, The continental record and the generation of continental crust: Geological Society of America Bulletin, v. 125, p. 14–32, doi:10.1130/B30722.1.

Cecil, R., Gehrels, G., Patchett, J., and Ducea, M., 2011, U-Pb-Hf characterization of the central Coast Mountains batholith: Implications for petrogenesis and crustal architecture: Lithosphere, v. 3, p. 247–260, doi:10.1130/L134.1.

Colpron, M., and Nelson, J., 2007, Northern Cordilleran terranes and their interactions through time: GSA Today, v. 17, no. 4/5, p. 4–10, doi:10.1130/GSAT01704-5A.1.

Colpron, M., and Nelson, J., 2009, A Palaeozoic Northwest Passage: Incursion of Caledonian, Baltican and Siberian terranes into eastern Panthalassa, and the early evolution of the North American Cordillera, *in* Cawood, P.A. and Kroner, A., eds., Earth Accretionary Systems in Space and Time: Geological Society of London Special Publication 318, p. 273–307.

Condie, K.C., Bickford, M.E., Aster, R.A., Belousova, E., and Scholl, D.W., 2011, Episodic zircon ages, Hf isotopic composition, and the preservation of continental crust: Geological Society of America Bulletin, v. 123, p. 951–957, doi:10.1130/B30344.1.

Dickinson, W.R., and Gehrels, G.E., 2008, U-Pb ages of detrital zircons in relation to paloegeography: Triassic paleodrainage networks and sediment dispersal across southwest Laurentia: Journal of Sedimentary Research, v. 78, p. 745–764, doi:10.2110/jsr.2008.088.

Fedo, C.M., Sircombe, K., and Rainbird, R., 2003, Detrital zircon analysis of the sedimentary record, *in* Hanchar J.M., and Hoskin, P.W.O., eds., Zircon: Reviews in Mineralogy and Geochemistry, v. 53, p. 277–303.

Flowerdew, M.J., Chew, D.M., Daly, J.S., and Millar, I.L., 2009, Hidden Archaean and Palaeoproterozoic crust in NW Ireland? Evidence from zircon Hf isotopic data from granitoid intrusions: Geological Magazine, v. 146, p. 903–916, doi:10.1017/S0016756809990227.

Furlanetto, F., Thorkelson, D.J., Davis, W.J., Hibson, H.D., Rainbird, R.H., and Marshall, D.D., 2009, Preliminary results of detrital zircon geochronology, Wernecke Supergroup, Yukon, *in* Weston, L.H., Blackburn, L.R., and Lewis L.L., eds., Yukon Exploration and Geology 2008: Yukon Geological Survey, p. 125–135.

Gehrels, G.E., 2000, Introduction to detrital zircon studies of Paleozoic and Triassic strata in western Nevada and northern California, *in* Gehrels, G.E., and Soreghan, M.J., eds., Paleozoic and Triassic Paleogeography and Tectonics of Western Nevada and Northern California: Boulder, Colorado, Geological Society of America, Special Paper 347, p. 1–17, doi:10.1130/0-8137-2347-7.1.

Gehrels, G.E., and Dickinson, W.R., 1995, Detrital zircon provenance of Cambrian to Triassic miogeoclinal and eugeoclinal strata in Nevada: American Journal of Science, v. 295, p. 18–48, doi:10.2475/ajs.295.1.18.

Gehrels, G.E., and Dickinson, W.R., 2000, Detrital zircon geochronology of the Antler overlap and foreland basin assemblages, Nevada, *in* Gehrels, G.E., and Soreghan, M.J., eds., Paleozoic and Triassic Paleogeography and Tectonics of Western Nevada and Northern California: Boulder, Colorado, Geological Society of America, Special Paper 347, p. 57–63, doi:10.1130/0-8137-2347-7.57.

Gehrels, G.E., and Ross, G.M., 1998, Detrital zircon geochronology of Neoproterozoic to Permian miogeoclinal strata in British Columbia and Alberta: Canadian Journal of Earth Sciences, v. 35, p. 1380–1401, doi:10.1139/e98-071.

Gehrels, G.E., and Stewart, J.H., 1998, Detrital zircon geochronology of Cambrian to Triassic miogeoclinal and eugeoclinal strata of Sonora, Mexico: Journal of Geophysical Research, v. 103, p. 2471–2487, doi:10.1029/97JB03251.

Gehrels, G.E., Dickinson, W.R., Ross, G.M., Stewart, J.H., and Howell, D.G., 1995, Detrital zircon reference for Cambrian to Triassic miogeoclinal strata of western North America: Geology, v. 23, p. 831–834, doi:10.1130/0091-7613(1995)023<0831:DZRFCT>2.3.CO;2.

Gehrels, G.E., Butler, R.F., and Bazard, D.R., 1996, Detrital zircon geochronology of the Alexander terrane, southeastern Alaska: Geological Society of America Bulletin, v. 108, p. 722–734, doi:10.1130/0016-7606(1996)108<0722:DZGOTA>2.3.CO;2.

Gehrels, G.E., Johnsson, M.J., and Howell, D.G., 1999, Detrital zircon geochronology of the Adams Argillite and Nation River Formation, east-central Alaska: Journal of Sedimentary Research, v. 69, p. 135–144, doi:10.2110/jsr.69.135.

Gehrels, G.E., Dickinson, W.R., Riley, B.C.D., Finney, S.C., and Smith, M.T., 2000a, Detrital zircon geochronology of the Roberts Mountains allochthon, Nevada, *in* Gehrels, G.E., and Soreghan, M.J., eds., Paleozoic and Triassic Paleogeography and Tectonics of Western Nevada and Northern California: Boulder, Colorado, Geological Society of America, Special Paper 347, p. 19–42, doi:10.1130/0-8137-2347-7.19.

Gehrels, G.E., and 13 others, 2000b, Tectonic implications of detrital zircon data from Paleozoic and Triassic strata in western Nevada and northern California, *in* Gehrels, G.E., and Soreghan, M.J., eds., Paleozoic and Triassic Paleogeography and Tectonics of Western Nevada and Northern California: Boulder, Colorado, Geological Society of America, Special Paper 347, p. 133–150, doi:10.1130/0-8137-2347-7.133.

Gehrels, G., Blakey, R., Karlstrom, K., Timmons, M., Dickinson, W., and Pecha, M., 2011, Detrital zircon U-Pb geochronology of Paleozoic strata in the Grand Canyon: Lithosphere, v. 3, p. 183–200, doi:10.1130/L121.1.

González-León, C.M., Stanley, G.D., Gehrels, G.E., and Centeno, E., 2005, New data on the lithostratigraphy, detrital zircon and Nd isotope provenance, and paleogeographic setting of the El Antimonio Group, Sonora, Mexico, *in* Anderson, T.H., Nourse, J.A., McKee, J.W., and Steiner, M.B., eds., 2005, The Mojave-Sonora Megashear Hypothesis: Development, Assessment, and Alternatives: Boulder, Colorado, Geological Society of America, Special Paper 393, p. 259–282, doi:10.1130/0-8137-2393-0.259.

Goodge, J.W., and Vervoort, J.D., 2006, Origin of Mesoproterozoic A-type granites in Laurentia: Hf isotopic evidence: Earth and Planetary Science Letters, v. 243, p. 711–731, doi:10.1016/j.epsl.2006.01.040.

Hadlari, T., Davis, W.J., Dewing, K., Heaman, L.M., Lemieux, Y., Ootes, L., Pratt, B.R., and Pyle, L.J., 2012, Two detrital zircon signatures for the Cambrian passive margin of northern Laurentia highlighted by new U-Pb results from northern Canada: Geological Society of America Bulletin, v. 124, p. 1155–1168, doi:10.1130/B30530.1.

Haq, B.U., and Schutter, S.R., 2008, A chronology of Paleozoic sea-level changes: Science, v. 322, p. 64–68, doi:10.1126/science.1161648.

Hawkesworth, C.J., Dhuime, B., Pietranik, A.B., Cawood, P.A., Kemp, A.I.S., and Storey, C.D., 2010, The generation and evolution of the continental crust: Journal of the Geological Society, v. 167, p. 229–248, doi:10.1144/0016-76492009-072.

Hoffman, P.F., 1989, Precambrian geology and tectonic history of North America, *in* Bally, A.W., and Palmer, A.R., eds., The Geology of North America: An Overview: Boulder, Colorado, Geological Society of America, The Geology of North America, v. A, p. 447–512.

Ketner, K.B., 1968, Origin of Ordovician Quartzite in the Cordilleran miogeosyncline, *in* Geological Survey Research 1968 Chapter B: U.S. Geological Survey Professional Paper 600-B, p. 169–177.

Ketner, K.B., 1986, Eureka Quartzite in Mexico?—Tectonic implications: Geology, v. 14, p. 1027–1030, doi:10.1130/0091-7613(1986)14<1027:EQIMI>2.0.CO;2.

Kluth, C.F., and Coney, P.J., 1981, Plate tectonics of the Ancestral Rocky Mountains: Geology, v. 9, p. 10–15, doi:10.1130/0091-7613(1981)9<10:PTOTAR>2.0.CO;2.

Lawton, T.F., Hunt, G.J., and Gehrels, G.E., 2010, Detrital zircon record of thrust belt unroofing in Lower Cretaceous synorogenic conglomerates, central Utah: Geology, v. 38, p. 463–466, doi:10.1130/G30684.1.

Lemieux, Y., Hadlari, T., and Simonetti, A., 2011, Detrital zircon geochronology and provenance of Devono-Mississippian strata in the northern Canadian Cordilleran miogeocline: Canadian Journal of Earth Sciences, v. 48, p. 515–541.

Link, P.K., Fanning, C.M., and Beranek, L.P., 2005, Reliability and longitudinal change of detrital-zircon age spectra in the Snake River system, Idaho and Wyoming: An example of reproducing the bumpy barcode: Sedimentary Geology, v. 182, p. 101–142, doi:10.1016/j.sedgeo.2005.07.012.

McKerrow, W.S., Niocaill, C.M., and Dewey, J.F., 2000, The Caledonian Orogeny redefined: Journal of the Geological Society, v. 157, p. 1149–1154, doi:10.1144/jgs.157.6.1149.

Miller, E., Toro, J., Gehrels, G., Amato, J., Prokopiev, A., Tuchkova, M., Akinin, V., Dumitru, T., Moore, T., Embry, A., and Cecile, M., 2006, New insights into Arctic paleogeography and tectonics from U-Pb detrital zircon geochronology: Tectonics, v. 25, TC3013, doi:10.1029/2005TC001830.

Miller, E.L., Gehrels, G.E., Pease, V., and Sokolov, S., 2010, Stratigraphy and U-Pb detrital zircon geochronology of Wrangel Island, Russia: Implications for Arctic paleogeography: The American Association of Petroleum Geologists Bulletin, v. 94, p. 665–692, doi:10.1306/10200909036.

Mueller, P., Foster, D., Mogk, D., Wooden, J., and Vogl, J., 2007, Detrital mineral chronology of the Uinta

Mountain Group: Implications of the Grenville flood in southwestern Laurentia: Geology, v. 35, p. 431–434, doi:10.1130/G23148A.1.

Mueller, P.A., Kamenov, G.D., Heatherington, A.L., and Richards, J., 2008, Crustal evolution in the southern Appalachian orogen: Evidence from Hf isotopes in detrital zircons: The Journal of Geology, v. 116, p. 414–422, doi:10.1086/589311.

Patchett, P.J., and Chase, C.G., 2002, Role of transform continental margins in major crustal growth episodes: Geology, v. 30, p. 39–42, doi:10.1130/0091-7613 (2002)030<0039:ROTCMI>2.0.CO;2.

Patchett, P.J., Ross, G.M., and Gleason, J.D., 1999, Continental drainage in North America during the Phanerozoic from Nd isotopes: Science, v. 283, p. 671–673, doi:10.1126/science.283.5402.671.

Poole, F.G., Gehrels, G.E., and Stewart, J.H., 2008, Significance of detrital zircons in Upper Devonian ocean-basin strata of the Sonora allochthon and Lower Permian synorogenic strata of the Mina Mexico foredeep, central Sonora, Mexico, *in* Blodgett, R.B., and Stanley, G.D., eds., The Terrane Puzzle: New Perspectives on Paleontology and Stratigraphy from the North American Cordillera: Boulder, Colorado, Geological Society of America, Special Paper 442, p. 121–131.

Rainbird, R.H., Heaman, L.M., and Young, G., 1992, Sampling Laurentia: Detrital zircon geochronology offers evidence for an extensive Neoproterozoic river system originating from the Grenville orogen: Geology, v. 20, p. 351–354, doi:10.1130/0091-7613(1992)020<0351: SLDZGO>2.3.CO;2.

Rainbird, R., Cawood, P., and Gehrels, G., 2012, The great Grenvillian sedimentation episode: Record of supercontinent Rodinia's assembly, *in* Busby, C., and Azor, A., eds., Tectonics of Sedimentary Basins: Recent Advances: Chichester, West Sussex, UK, Wiley-Blackwell Publishing, p. 583–601.

Riggs, N.R., Lehman, T.M., Gehrels, G.E., and Dickinson, W.R., 1996, Detrital zircon link between headwaters and terminus of the Upper Triassic Chinle-Dockum paleoriver system: Science, v. 273, p. 97–100, doi: 10.1126/science.273.5271.97.

Riggs, N.R., Barth, A.P., González-León, C.M., Jacobson, C.E., Wooden, J.L., Howell, E.R., and Walker, J.D., 2012, Provenance of Upper Triassic strata in southwestern North America as suggested by isotopic analysis and chemistry of zircon crystals, *in* Rasbury, E.T., Hemming, S.R., and Riggs, N.R., eds., Mineralogical and Geochemical Approaches to Provenance: Boulder, Colorado, Geological Society of America, Special Paper 487, p. 13–36, doi:10.1130/2012.2487(02).

Roberts, N.M.W., 2012, Increased loss of continental crust during supercontinent amalgamation: Gondwana Research, v. 21, p. 994–1000, doi:10.1016 /j.gr.2011.08.001.

Rohr, T.S., Andersen, T., and Dypvik, H., 2008, Provenance of Lower Cretaceous sediments in the Wandel Sea Basin, North Greenland: Journal of the Geological Society, v. 165, p. 755–767, doi:10.1144/0016 -76492007-102.

Rohr, T.S., Andersen, T., Dypvik, H., and Embry, A.F., 2010, Detrital zircon characteristics of the Lower Cretaceous Isachsen Formation, Sverdrup Basin: Source constraints from age and Hf isotope data: Canadian Journal of Earth Sciences, v. 47, p. 255–271, doi:10.1139 /E10-006.

Ross, G.M., 1991, Precambrian basement in the Canadian Cordillera: An introduction: Canadian Journal of Earth Sciences, v. 28, p. 1133–1139, doi:10.1139/e91-103.

Ross, G.M., 2002, Evolution of Precambrian continental lithosphere in western Canada: Results from Lithoprobe studies in Alberta and beyond: Canadian Journal of Earth Sciences, v. 39, p. 413–437, doi:10.1139 /e02-012.

Ross, G.M., and Parrish, R.R., 1991, Detrital zircon geochronology of metasedimentary rocks in the southern Omineca Belt, Canadian Cordillera: Canadian Journal of Earth Sciences, v. 28, p. 1254–1270, doi:10.1139 /e91-112.

Ross, G.M., Gehrels, G.E., and Patchett, P.J., 1997, Provenance of Triassic strata in the Cordilleran miogeocline, western Canada: Bulletin of the Canadian Society of Petroleum Geologists, v. 45, p. 461–473.

Shufeldt, O., Karlstrom, K., Gehrels, G., and Howard, K., 2010, Archean detrital zircons in the Proterozoic Vishnu Schist of the Grand Canyon, Arizona: Implications for crustal architecture and Nuna supercontinent reconstructions: Geology, v. 38, p. 1099–1102, doi: 10.1130/G31335.1.

Sircombe, K.N., 2000, Reading the bumpy barcode: Quantification and interpretation of detrital geochronology data with provenance study examples from modern beach sands and Archean metasedimentary rocks: Geological Society of America Abstracts with Programs, v. 32, no. 6, p. 68.

Sloss, L.L., 1988, Tectonic evolution of the craton in Phanerozoic time, *in* Sloss, L.L., ed., Sedimentary Cover—North American Craton: Boulder, Colorado, Geological Society of America, The Geology of North America, v. D-2, p. 25–51.

Smith, M.T., and Gehrels, G.E., 1994, Detrital zircon geochronology and the provenance of the Harmony and Valmy Formations, Roberts Mountains allochthon, Nevada: Geological Society of America Bulletin, v. 106, p. 968–979, doi:10.1130/0016-7606(1994)106 <0968:DZGATP>2.3.CO;2.

Soja, C.M., 1994, Significance of Silurian stromatolite-sphinctozoan reefs: Geology, v. 22, p. 355–358, doi:10.1130/0091-7613(1994)022<0355:SOSSSR>2.3 .CO;2.

Stevenson, R.K., Whittaker, S., and Mountjoy, E.W., 2000, Geochemical and Nd isotopic evidence for sedimentary-source changes in the Devonian miogeocline of the southern Canadian Cordillera: Geological Society of America Bulletin, v. 112, p. 531–539, doi:10.1130 /0016-7606(2000)112<531:GANIEF>2.0.CO;2.

Stewart, J.H., 1976, Late Precambrian evolution of North America: Plate tectonics explanation: Geology, v. 4, p. 11–15, doi:10.1130/0091-7613(1976)4<11: LPEONA>2.0.CO;2.

Stewart, J.H., Gehrels, G.E., Barth, A.P., Link, P.K., Christie-Blick, N., and Wrucke, C.T., 2001, Detrital zircon provenance of Mesoproterozoic to Cambrian arenites in the western United States and northwestern Mexico: Geological Society of America Bulletin, v. 113, p. 1343–1356, doi:10.1130/0016-7606 (2001)113<1343:DZPOMT>2.0.CO;2.

Vervoort, J., 2011, The caveats in the use of Hf model ages in provenance (and other) studies: Geological Society of America Abstracts with Programs, v. 43, no. 5, p. 206.

Vervoort, J.D., and Blichert-Toft, J., 1999, Evolution of the depleted mantle: Hf isotope evidence from juvenile rocks through time: Geochimica et Cosmochimica Acta, v. 63, p. 533–556, doi:10.1016/S0016-7037 (98)00274-9.

Vervoort, J.D., and Patchett, P.J., 1996, Behavior of hafnium and neodymium isotopes in the crust: Constraints from crustally derived granites: Geochimica et Cosmochimica Acta, v. 60, p. 3717–3733, doi:10.1016/0016 -7037(96)00201-3.

Vervoort, J.D., Patchett, P.J., Blichert-Toft, J., and Albarede, F., 1999, Relationships between Lu-Hf and Sm-Nd isotopic systems in the global sedimentary system: Earth and Planetary Science Letters, v. 168, p. 79–99, doi: 10.1016/S0012-821X(99)00047-3.

Wallin, E.T., Noto, R.C., and Gehrels, G.E., 2000, Provenance of the Antelope Mountain Quartzite, Yreka Terrane, California: Evidence for large-scale late Paleozoic sinistral displacement along the North American Cordilleran margin and implications for the mid-Paleozoic fringing-arc model, *in* Soreghan, M.J. and Gehrels, G.E., eds., Paleozoic and Triassic Paleogeography and Tectonics of Western Nevada and Northern California: Boulder, Colorado, Geological Society of America, Special Paper 347, p. 119–132, doi:10.1130/0-8137 -2347-7.119.

Whitmeyer, S.J., and Karlstrom, K.E., 2007, Tectonic model for the Proterozoic growth of North America: Geosphere, v. 3, p. 220–259, doi:10.1130/GES00055.1.

Wooden, J.L., Barth, A.P., and Mueller, P.A., 2013, Crustal growth and tectonic evolution of the Mojave crustal province: Insights from hafnium isotope systematics in zircons: Lithosphere, v. 5, p. 17–28, doi:10.1130/L218.1.

Wright, J., and Wyld, S., 2006, Gondwana, Iapetan, Cordilleran interactions: A geodynamic model for the Paleozoic tectonic evolution of the North American Cordillera, *in* Haggart, J., Enkin, R., and Monger, J., eds., Paleogeography of the North American Cordillera: Evidence For and Against Large-Scale Displacements: Geological Association of Canada Special Paper 46, p. 377–408.